Astron. Astrophys. 294, 469–487 (1995)

ASTRONOMY AND ASTROPHYSICS

# On the evolution of rotational velocity distributions for solar-type stars

**R. Keppens**[1,2*], **K.B. MacGregor**[1**], **and P. Charbonneau**[1]

[1] High Altitude Observatory, National Center for Atmospheric Research, 3450 Mitchell Lane Bldg. 2, Boulder, CO 80301, USA
[2] Center for Plasma-Astrophysics, K.U.L., Departement Wiskunde, Celestijnenlaan 200B, B-3001 Heverlee, Belgium

Received 19 March 1994 / Accepted 13 August 1994

**Abstract.** We investigate how the distribution of rotational velocities for late-type stars of a given mass evolves with age, both before and during residence on the main sequence. Starting from an age $\sim 10^6$ years, an assumed pre-main sequence rotational velocity/period distribution is evolved forward in time using the model described by MacGregor & Brenner (1991) to trace the rotational histories of single, constituent stars. This model treats: (i) stellar angular momentum loss as a result of the torque applied to the convection zone by a magnetically coupled wind; (ii) angular momentum transport from the radiative interior to the convective envelope in response to the rotational deceleration of the stellar surface layers; and (iii), angular momentum redistribution associated with changes in internal structure during the process of contraction to the main sequence.

We ascertain how the evolution of a specified, initial rotational velocity/period distribution is affected by such things as: (i) the dependence of the coronal magnetic field strength on rotation rate through a prescribed, phenomenological dynamo relation; (ii) the magnitude of the timescale $\tau_c$ characterizing the transfer of angular momentum from the core to the envelope; (ii) differences in the details and duration of pre-main sequence structural evolution for stars with masses in the range $0.8 \leq M_*/M_\odot \leq 1.0$; and (iv), the exchange of angular momentum between a star and a surrounding, magnetized accretion disk during the first few million years of pre-main sequence evolution following the development of a radiative core. The results of this extensive parameter study are compared with the distributions derived from measurements of rotational velocities of solar-type stars in open clusters with known ages. Starting from an initial distribution compiled from observations of rotation among T Tauri stars, we find that reasonable agreement with the distribution evolution inferred from cluster observations is obtained for: (i) a dynamo law in which the strength of the coronal field increases linearly with surface angular velocity for rotation rates $\leq 20$ times the present solar rate, and becomes saturated for more rapid rotation; (ii) a coupling timescale $\sim 10^7$ years; (iii) a mix of stellar masses consisting of roughly equal numbers of 0.8 $M_\odot$ and 1.0 $M_\odot$ stars; and (iv), disk regulation of the surface rotation up to an age $\sim 6 \times 10^6$ years for stars with initial rotation periods longer than 5 days. A number of discrepancies remain, however: even with the most favorable choice of model parameters, the present calculations fail to produce a sufficiently large proportion of slow (equatorial velocities less than 10 kms$^{-1}$) rotators on the Zero-Age Main Sequence.

**Key words:** accretion, accretion disks – stars: evolution – stars: magnetic fields – stars: mass-loss – stars: rotation of

## 1. Introduction

Clues to understanding the rotational history of a star like the sun are mainly gathered from observations of stars in clusters of different ages. The youngest such stars observed are only a few million years old, and are still contracting toward the Zero-Age Main Sequence (ZAMS). Surveys of rotation among low mass Pre-Main Sequence (PMS) stars aim to get an idea of the initial angular momentum distribution for solar-type stars. Spectroscopic determinations of rotational velocities, projected onto the line of sight ($v \sin i$), are available for more than a hundred T Tauri stars (TTS, i.e., low mass stars of age less than $10^7$ yrs; Bouvier 1991 and references therein). The average rotational velocity of a young solar mass star is about 15 kms$^{-1}$, or a 6.7 day period assuming a stellar radius $R_* = 2R_\odot$. Photometric campaigns help to determine true rotational periods, when the variability in stellar lightcurves can be satisfactorily modelled in terms of rotational modulation (e.g., by starspots). Results obtained by photometric monitoring of TTS in the Orion Nebulae Cluster (Attridge & Herbst 1992) are suggestive of a bimodal distribution of rotation periods. The sample surveyed shows a slow rotator group (with a mean period of 8.5 days and a 2.5 days dispersion) and a rapid rotator group (mean period

*Send offprint requests to*: R. Keppens (H.A.O., N.C.A.R.)

* Research Assistant of the Belgian National Fund of Scientific Research

** The National Center for Atmospheric Research is sponsored by the National Science Foundation

2.2 days and a 1 day dispersion). Similarly, the COYOTES I campaign (Bouvier et al. 1993), monitoring TTS in the Taurus-Auriga cloud, shows evidence for both rapid and slow rotators. The apparent bimodality of the period distribution has been interpreted as being a consequence of the interaction between a contracting, PMS star and a surrounding, magnetized accretion disk. This interaction, presumed magnetic in origin, is yet to be modeled quantitatively (see Hoyle 1960, for some pioneering ideas on this interaction in the context of the Solar Nebula). Slowly rotating Classical T Tauri Stars (CTTS) show evidence for the presence of disks, while the more rapidly rotating, Weak-line T Tauri Stars (WTTS) do not. At an age $\sim 10^6$ years, the fraction of stars with disks is of order 50%, and this fraction decreases to less than 10% at 10 Myr (e.g. Stauffer 1994 and references therein).

When a reliable determination of the initial period distribution is made, the challenge for any rotational evolution calculation is to provide a scenario for the evolution of the distribution that agrees with the results obtained from observations of clusters of known ages. In Fig. 1, we show the observed $v \sin i$ distributions[1] of solar-type stars ($B - V$ color indices between 0.55-0.85, corresponding to a mass range of about $M_* = 1.0 - 0.8 M_\odot$) for the $\alpha$ Persei cluster (age 50 Myr), the Pleiades (age 70 Myr) and the Hyades cluster (age 600 Myr). Although the sample sizes of the distributions presented are rather small (47 stars for $\alpha$ Persei, 72 for the Pleiades and only 29 for the Hyades), we can deduce some of the properties of the evolution of stellar rotation during the early stages of the Main Sequence (MS) lifetime. We note that this is only meaningful if we assume that the current TTS observations are representative of the period distribution of $\alpha$ Persei, Pleiades and Hyades at earlier times. A considerable spread in rotation rates is clearly present for stars in the $\alpha$ Persei cluster. Roughly two thirds of the stars observed have rotational velocities less than 30 kms$^{-1}$. In particular, we note the large population of stars in the 0-10 kms$^{-1}$ bin (which also contains stars with a known upper limit of 10 kms$^{-1}$). The remaining third of the distribution with rotational velocities higher than 30 kms$^{-1}$ shows a continuous range of rotational velocities tailing out to 200 kms$^{-1}$. With the inevitable uncertainties on the cluster's age and intrinsic age spread, one may infer that the period distributions for young MS stars should show these two properties: an elongated tail out to extremely fast rotation rates, and a considerable fraction (roughly 2/3) of objects rotating slower than 30 kms$^{-1}$. With an adopted age difference of 20 Myr between $\alpha$ Persei and the Pleiades, the rotational distribution of stars in the Pleiades implies that considerable spin-down occurs within a few $10^7$ yrs. About 80-90 % of all stars in this cluster are rotating with $V_{eq} < 30$ kms$^{-1}$, and for the sample shown, the maximal rotation is only 100 kms$^{-1}$, suggestive of a 50 % spin-down of the most rapidly rotating stars in about 20 Myr. Note that the Pleiades data already show half of the stars rotating slower than

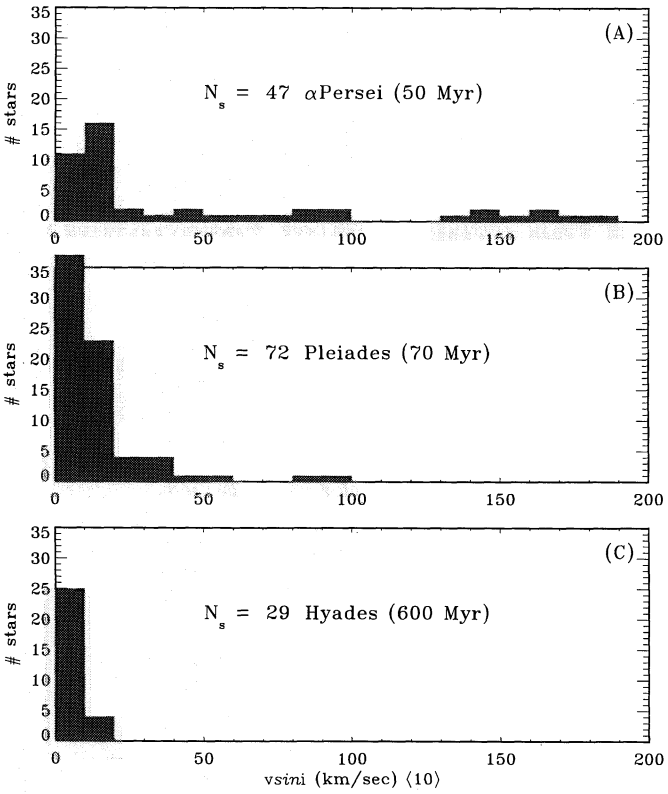


**Fig. 1a–c.** Observed $v \sin i$ distributions for three clusters of known age, using data from Soderblom et al. 1993: **a** $\alpha$ Persei (50 Myr); **b** Pleiades (70Myr); **c** Hyades (600 Myr). Only stars with $B - V$ color index between 0.55-0.85 (or mass $0.8 M_\odot$-$1.0 M_\odot$) are shown. The velocity bins have width 10 kms$^{-1}$. When a star's rotation is known as an upper limit, we put its $v \sin i$ value in the appropriate bin

10 kms$^{-1}$. At the age of the Hyades (600 Myr), all solar-type stars have rotational velocities typically below 10 kms$^{-1}$. Consistent modeling of the evolution of the rotational velocity distribution thus has to account for: (i) sufficient slow rotators and (ii) a tail of fast rotators in the late-PMS/early-MS evolution; (iii) rapid spin-down of the fastest rotators; and (iv) explain how all stars end up slowly rotating after several hundred Myrs.

In this paper, we present a basic scenario for the rotational evolution of a solar-type star, and calculate the evolution of an initial period distribution for low mass stars in accord with this scenario. We intend to demonstrate the effect of the different physical parameters that enter our model, and this parameter study will eventually lead to a suitable model calculation that qualitatively recovers the observed evolution of the distribution of rotational velocity. Recent papers on the rotational evolution of stars have noted the difficulties arising when trying to model all evolutionary properties suggested by the observations. Bouvier (1994) discussed how a large spread in rotational velocity at ZAMS ages results from strong PMS spin up for rigidly rotating stars, and how braking of TTS, while they are magnetically coupled to a circumstellar disk, explains the coexistence of the slower rotators at those ages. We elaborate on these ideas, using a less restrictive model for the stellar structural and rotational

[1] Data taken from a variety of sources, as in Soderblom et al. 1993, Fig. 1; updated with recent observations by Prosser 1994: all $B - V$ color indices are corrected for reddening by a 'mean' factor of 0.1.

evolution (as opposed to rigid rotation) and physically more adequate braking laws. Li & Collier Cameron (1993) used a two-component model to calculate the MS rotational evolution of a solar-type star, wherein both the radiative core and the convective envelope are assumed to rotate rigidly. If these two regions were weakly coupled, a reasonable fit to the MS evolution of the distribution of rotational velocities was provided. While, in principle, our calculations use a similar model, we will argue for stronger effective coupling between the core and the envelope. This apparent disagreement is partly due to the range in rotational velocities that Li & Collier Cameron adopted for the Pleiades cluster: the maximum rotational velocity in this cluster was assumed to be 40 $\mathrm{kms}^{-1}$ (more rapid rotators have been observed, see Fig. 1), which required a fast spin-down to occur between the ages of $\alpha$ Persei and the Pleiades. Soderblom et al. (1993) presented the evolution of an initial early-PMS (2 Myr) distribution of rotational velocities up to 50 $\mathrm{kms}^{-1}$. They used the MacGregor & Brenner (1991) formalism for the evolution of a single star, in which the structural evolution of the core and the convective envelope, together with angular momentum redistribution and loss, are consistently incorporated in PMS/MS rotational evolution. We will use the same formalism, with a more accurate description of the angular momentum loss from the stellar wind as the structural evolution influences the stellar gravitation, rotation and magnetization. Additionally, and in accord with Bouvier (1994), we will schematically account for the influence of circumstellar accretion disks in the star's magnetosphere.

The basic scenario for the rotational evolution of a single star is as follows. During PMS evolution, the overall contraction and internal structural changes cause the star to spin up. A radiative core develops, and this core ends up rotating faster than the (convective) envelope. Rapid surface rotation in late-PMS/early-MS evolution is expected when the coupling between the radiative core and the convective envelope is efficient enough to ensure a continuous supply of angular momentum from the core to the envelope, thus limiting the degree of differential rotation that would otherwise develop. However, we also show that in the late-PMS/early-MS evolution, the influence of the stellar wind becomes crucial to the subsequent rotational evolution. The loss of angular momentum through a stellar wind retards and eventually halts the spin-up of the outer convection zone late in the PMS phase, and then continues to slow the stellar rotation. When the wind braking timescale is the shortest timescale involved, the convection zone undergoes a fast spin-down. The timescale for angular momentum loss through the stellar wind decreases with increasing rotation rate, and is quite sensitive to the coronal magnetic field strength. How this mean coronal field depends in detail on the star's rotation is largely unknown, but a specified parametric dynamo prescription $B_*(\Omega_*)$ (with $\Omega_*$ the stellar rotation rate) can be constructed and adjusted to fit the observations. When the stellar dynamo is believed to saturate at a certain rotation rate (i.e. the mean stellar coronal field does not increase with faster rotation), the loss of angular momentum through the stellar wind is reduced at faster rotation (as compared to the linear dynamo angular momentum loss rate), and the angular momenta of both core and envelope evolve quite gradually, with a continous decrease in the rotation rate of both regions throughout the MS lifetime. When no such saturation occurs, the convection zone initially spins down quickly and thus a large degree of differential rotation develops that is most obvious at about the time of arrival on the ZAMS. As soon as the difference in rotation between core and envelope causes an appreciable resupply of angular momentum to the outer convective layer by the visco-magnetic coupling mechanisms, a gradual spin-down of both regions occurs during subsequent MS evolution.

With this scenario for the rotational evolution of a single star, it is possible to explain how a reasonable spread in the initial period distribution can lead to rotation rates at the ZAMS ranging from moderate to fast. How long such large spreads in rotation rates are sustained, and how fast spin-down occurs, is then predicted by the model calculations, and is shown to be in reasonable accord with the observations (50 % spin-down in early MS, and rotation slower than 10 $\mathrm{kms}^{-1}$ at the Hyades age, 600 Myr). The evolution of the distribution of rotational velocities, as suggested by Fig. 1, can qualitatively be recovered when the coronal field saturates at a sufficiently high rotation rate, and/or when effective coupling between the core and envelope occurs.

From our model calculations for the evolution of the period distribution, we find that the most challenging problem is to account for a significant fraction of rotators with $V_{eq} < 30\ \mathrm{kms}^{-1}$ at about 50 Myrs (2/3 for the $\alpha$ Persei cluster) and 70 Myrs (with 50 % slower than 10 $\mathrm{kms}^{-1}$ in the Pleiades). We find that this fact can most easily be explained when part of the initial distribution is forced to remain in a state of slow rotation for a few million years in the early PMS, as suggested by the bimodal period distribution of TTS. When the rotation rate of a low mass star is prevented from increasing as fast as the normal structural changes would imply for a few million years in the early PMS evolution, the star never reaches high rotational velocities (equatorial velocities less than 20 $\mathrm{kms}^{-1}$ throughout its evolution). We illustrate these arguments with simple calculations showing the relative importance of different parametric prescriptions for core-envelope coupling, dynamo saturation and disk regulation on the period distributions at relevant ages.

The paper is organized as follows: in Sect. 2, we introduce and discuss the equations describing the angular momentum evolution of a solar-type star. We show how the model parameters influence the rotational evolution of a single star. In Sect. 3, we calculate the predicted period distributions of representative star samples, and compare the results with the observed $v \sin i$ distributions. We illustrate the effect of different dynamo prescriptions, coupling mechanisms, stellar masses and interaction with accretion disks. We summarize our results in Sect. 4.

## 2. Model parameters: the rotational evolution of a single star

The parametrized model (MacGregor & Brenner 1991; MacGregor 1991; Soderblom et al. 1993; MacGregor & Charbonneau 1994) we adopt to describe the rotational evolution of a single star decouples the calculation of the internal structural evo-

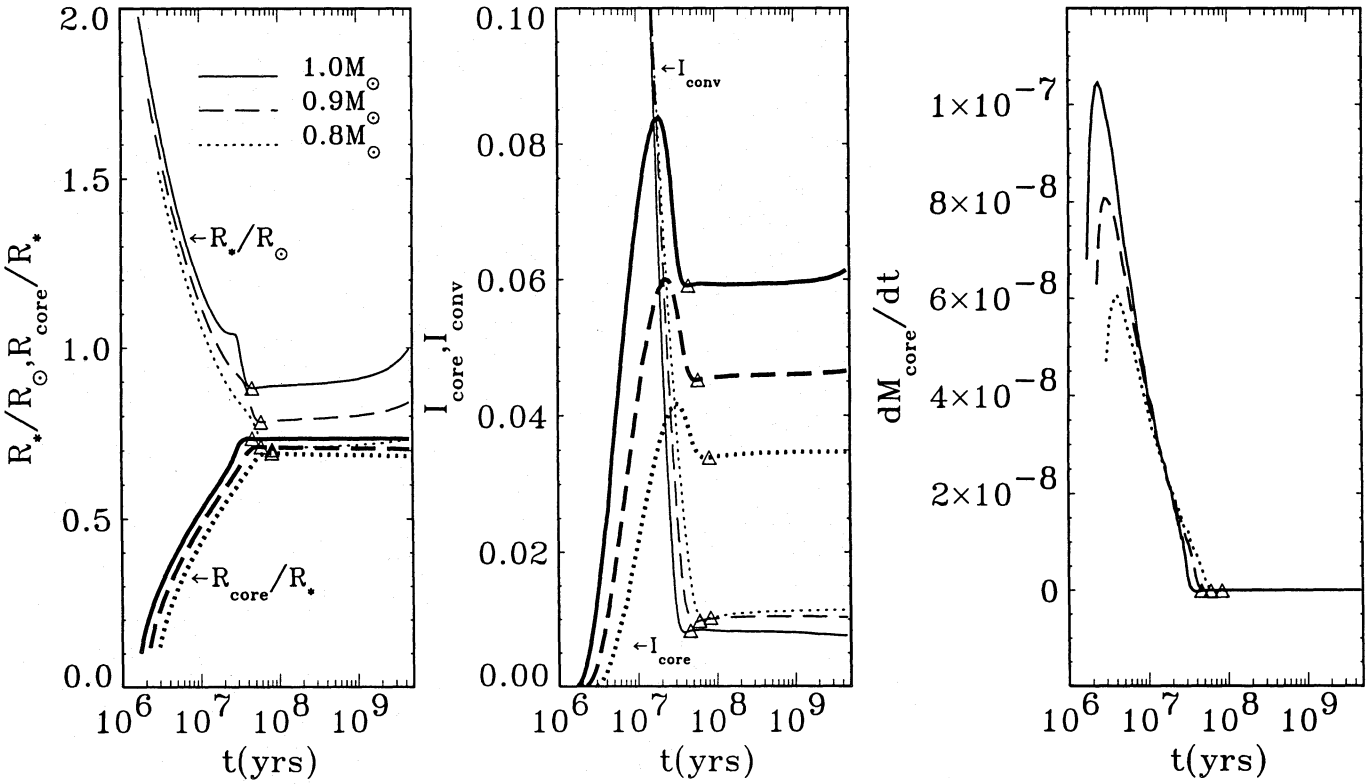


**Fig. 2.** Time evolution of stellar quantities for stars of mass 0.8 (dotted lines), 0.9 (dashed lines) and $1M_\odot$ (solid lines), from $t_{RC}$ to the solar age. Left: stellar radius (in $R_\odot$ units) and the core-convection zone boundary $R_{core}$ (in units of the star radius $R_*$ - thicker lines). Middle: Moment of inertia for core (thicker lines) and convection zone (in $10^{55}$ gcm$^2$ units). Right: the mass exchange rate $dM_{core}/dt$ at the core-convection zone boundary (mass in units of the star mass). Triangles denote the ZAMS. Data from evolutionary tracks provided by D. Vandenberg

lution from the calculation of the internal angular momentum redistribution and the angular momentum loss. Model calculations (e.g., Iben 1965) suggest that for solar-mass stars, collapse to a fully convective object with radius roughly two solar radii requires about two to three million years. Due to the ongoing contraction, the star then develops a radiative core. While the star keeps contracting to its minimal radius at the ZAMS, the core-convection zone boundary recedes outwards. This changing internal structure is accompanied by changes in the moments of inertia for the two regions (core and convective envelope) and a reapportioning of angular momentum between them at the boundary. Evolutionary tracks computed for non-rotating stars of fixed mass (kindly provided by D. Vandenberg) allow the determination of both the mass exchange rate $dM_{core}/dt$ at the boundary $R_{core}(t)$ between the core and the convective envelope, and the changing moments of inertia $I_{core}(t)$ and $I_{conv}(t)$ of the two regions. In Fig. 2, we present the time evolution of these quantities for stars of mass 0.8, 0.9 and $1M_\odot$. Less massive stars contract to smaller radii, with proportionately larger stellar envelopes with a bigger moment of inertia. The radiative core develops later in the structural evolution and postpones the onset of nuclear burning[2]. It is apparent from Fig. 2 that the MS structural evolution is almost negligible, and, in particular, no angular momentum reapportionment arising from mass exchange between core and envelope takes place.

We presume that both the core and envelope rotate rigidly[3], and solve for the time evolution of their respective angular momenta: $J_{core} = I_{core}\Omega_{core}$ and $J_{conv} = I_{conv}\Omega_{conv}$. For this purpose, we use conservation laws that consistently take account of: (i) the effect of the changing stellar structure on the angular momentum exchange at $R_{core}(t)$; (ii) the evolving moments of inertia; and (iii) changes in the angular momentum of core and envelope due to the torques exerted on each region separately. These torques result from magnetized stellar winds, from mass accretion from and magnetic interaction with a surrounding disk, and from mechanical coupling at the core-envelope interface. This latter coupling may result from viscous-like transport (e.g. Pinsonneault et al. 1989; Tassoul & Tassoul 1989), magnetic torques (e.g. Mestel & Weiss 1987; Charbon-

[2] The operational definition of ZAMS as that time where 99 % of the star's luminosity comes from the nuclear fusion process in the central core, almost coincides with the age of minimal stellar radius, denoted by the triangles in Fig. 2.

[3] Rigid rotation is a justifiable assumption when the internal angular momentum redistribution within each region (core and envelope) separately occurs much faster than the angular momentum exchange and loss between and from both regions. This is certainly the case for the Sun's convective envelope, but not necessarily within its radiative core.

neau & MacGregor 1993), and/or viscously-driven large-scale flows (e.g. Spiegel & Zahn 1992); henceforth we refer to it simply as 'visco-magnetic coupling'. In the absence of magnetic coupling with an accretion disk, the combination of these effects can be written down in the mathematical form (MacGregor 1991)

$$\frac{dJ_{core}}{dt} = -\frac{\Delta J}{\tau_c} + \frac{2}{3}\Omega_{conv} R^2_{core}(t)\frac{dM_{core}}{dt}, \quad (1)$$

for the core, and

$$\frac{dJ_{conv}}{dt} = \frac{\Delta J}{\tau_c} - \frac{2}{3}\Omega_{conv} R^2_{core}(t)\frac{dM_{core}}{dt} - \frac{J_{conv}}{\tau_w}, \quad (2)$$

for the convection zone.

In these equations, the timescales $\tau_c$ and $\tau_w$ are respectively, the coupling timescale parametrizing the visco-magnetic coupling mechanisms which act to eliminate differential rotation between the core and the envelope, and the spin-down timescale for angular momentum loss due to the (magnetized) stellar wind. Within the time $\tau_c$, we assume that the amount of angular momentum transferred from the core to the envelope is given by

$$\Delta J = \frac{J_{core} I_{conv} - J_{conv} I_{core}}{I_{core} + I_{conv}}. \quad (3)$$

The instantaneous exchange of angular momentum $\Delta J$ would equilibrate $\Omega_{core}$ and $\Omega_{conv}$ and thereby eliminate the unstable condition of a decrease in specific angular momentum with increasing distance from the rotation axis (e.g. Tassoul 1978).

The timescale associated with the stellar wind, $\tau_w$, needs to be calculated from a reasonable model for the steady-state expansion of the stellar corona. In our model, we use the Weber-Davis (1967, hereafter WD) prescription for the (1D) axisymmetric expansion of a polytropic, magnetized, rotating corona. We have calculated a WD solution for solar coronal conditions that reproduces many of the physical properties of the quiet solar wind (as described by Withbroe 1988), and then continued to construct a table of wind solutions for coronal field strengths and rotation rates ranging from 0.5 to 60 times the assumed solar values. The characteristics of the solar wind solution are described in Appendix A (see also MacGregor & Charbonneau 1994), together with a description on how the table of solutions can be used to incorporate the essential properties influencing the stellar wind, namely the stellar rotation, the stellar dynamo and coronal magnetic field, and the stellar gravitation. Incorporating gravitational changes arising from the structural evolution is particularly important when estimates for the mass loss and angular momentum loss during the PMS/early-MS are needed. During early PMS contraction, the dramatic changes in surface gravity dominate the wind properties, while later in the PMS evolution, and during the whole MS evolution, the star's rotation rate and its corresponding coronal field regulate $\tau_w$. The WD wind solutions for the range of field strengths and rotation rates given will lead to an overestimate of the applied braking torque, when the stellar magnetic field topology is greatly different from an overall (1D axisymmetric) radial magnetic field. In a dipolar field configuration, the closed field lines form a 'dead zone' from which no angular momentum is lost. Changes in the field topology due to a dynamo action that favors closed field lines are therefore not incorporated in this model, but could in principle be included, assuming a wind braking timescale $\tau_w$ that in some way reflects this change in field topology. At present, there are no real guidelines as to how such an effect could be modeled quantitatively (see however, Mestel & Spruit 1987). As the WD wind solutions are *exact solutions of the ideal MHD equations* for the assumed field geometry and coronal parameters, their use to characterize the wind of a star during its PMS/MS evolution leads to a more deterministic picture than ad hoc parametric characterizations of the wind braking law.

The conservation laws (Eqs.. (1)-(2)) form a set of two ODE's, to be solved numerically, with initial conditions

$$J_{core} = \Omega_s I_{core}(t_{RC}), \quad (4)$$

$$J_{conv} = \Omega_s I_{conv}(t_{RC}), \quad (5)$$

where $t_{RC}$ is the time at which a small central core starts to form (of the order of 2 Myr, see Fig. 2). The initial equatorial velocity $V_{eq}(t_{RC}) = \Omega_s R_*(t_{RC})$ is chosen within reasonable limits of the observed average of 15 $\mathrm{kms}^{-1}$ for a $1\mathrm{M}_\odot$ TT star (Bouvier 1991). We assume that the fully convective star rotated rigidly up to $t_{RC}$, and therefore adopt identical rotation rates ($\Omega_s$) for the small core and the envelope at this time.

When a disk is present, we assume that the applied torques on the convection zone balance to a constant equilibrium rotation period. This approximation is admittedly crude, and some further comment is necessary (see also Appendix B). The bimodality apparent in the period distributions of TT stars observed in the Orion Nebulae Cluster (Attridge & Herbst 1992) and Taurus Auriga (Bouvier et al. 1993), has been attributed by several authors to the presence of accretion disks in the stellar magnetospheres of the slower rotators (e.g. Attridge & Herbst 1992; Bouvier et al. 1993; Collier Cameron & Campbell 1993; Edwards et al. 1993; Bouvier 1994). The CTTS show evidence for mass accretion from surrounding disks in the form of excess (compared to the stellar effective temperature) infrared emission from the cold disk regions. When such disks are present, and if a magnetic coupling exists between the star and the accretion disk, a combination of torques are applied to the stellar convection zone. The mass accreting onto the stellar surface causes the star to spin up when it accretes from within the corotation radius where the local Keplerian rotation rate equals the surface rotation rate. In fact, an MHD flow is set up between this inner portion of the accretion disk and that portion of the stellar surface that is magnetically connected to this inner portion. In addition to angular momentum gain from mass accretion, the viscous and magnetic stresses that build up at the disk-magnetosphere interface apply spin-up torques to the star that are transported along magnetic field lines (Li 1994; see also Ghosh & Lamb 1979; Königl 1991). The outer portion of the stellar disk rotates slower than the stellar surface, and sets up corresponding spin-down torques. The spin-down is supplemented by the stellar wind, which may have very different properties than the simple

WD description assumes, through the mere existence of the accretion disk and the physical (MHD) processes occuring when accretion takes place. It can be argued however, that the net effect of all the applied torques is to keep the star's rotation rate lower than that of a similar, but diskless star of the same age. The most convincing argument to date is the apparent agreement of the bimodal period distribution in both Orion Nebulae Cluster and Taurus Auriga TT stars with the CTTS/WTTS distinction. The fact that the COYOTES I campaign (Bouvier et al. 1993) shows a Gaussian shaped distribution of rotational periods of CTTS, with a small scatter around the mean value of 7.6 days, is an indication that some equilibrium situation where the rotation period remains constant throughout the disk lifetime is not an unreasonable approximation. Further motivation for this crude 'torque balance' argument is obtained from approximate, yet suggestive calculations performed by Collier Cameron & Campbell (1993), who found their (convective) TT stars attaining a fairly constant equilibrium period when high accretion rates and/or strong magnetic fields combine to produce balancing torques. In Appendix B, we present a set of calculations based on the model of Collier Cameron & Campbell (1993) to follow the rotational evolution of a PMS star magnetically coupled to a surrounding accretion disk, from the time $t_{RC} \sim 2$ Myr at which a radiative core starts to form. With reasonable accretion rates, and photospheric field strengths of $\sim 10^2 - 10^3$ Gauss, it is found that disks influence the stellar rotation rate up to about 5 or more Myr, even though the accretion timescale is only taken to be 1 Myr. The net overall effect is to keep the rotation rate roughly constant during several Myr, which is the assumption adopted in this paper and previously advanced by Bouvier (1994).

In Fig. 3, we show the influence of the model parameters on the rotational evolution of a single star. The calculated rotation rates should be considered in conjunction with the structural evolution of the star, presented in Fig. 2. Panels a, b and c are calculated for a $1M_\odot$ star, and illustrate the effect of varying the coupling timescale, the dynamo prescription and the initial equatorial rotational velocity $V_{eq}$. In panel (D), we consider the rotational evolution of stars of different mass. It is apparent from Fig. 3 that the rotational memory of a solar-type star is entirely lost at the age of the present day sun ($t_\odot = 4.5$ billion years). All models considered end up rotating at nearly the present day solar rotation rate ($\Omega_\odot \approx 3 \times 10^{-6}\ s^{-1}$) with essentially no internal differential rotation. This is already a basic result for the rotational history of a solar-type star. We now continue to discuss each panel separately.

We first consider (Panel (A)) how the phenomenological dynamo prescription influences the rotational evolution of the star. The dynamo law relates the base coronal magnetic field strength to the star's rotation rate. Such a dependence can be expected when the stellar magnetic field is sustained by the interplay of convection and differential rotation, as in the case of the sun (the so-called $\alpha\omega$-dynamo). For moderate rotation (up to a few times $\Omega_\odot \approx 3\times 10^{-6} s^{-1}$), the strength of the mean field generated in this way increases with rotation. A linear dynamo law, given by

$$B_*/B_\odot = (\frac{R_*(t_\odot)}{R_*})^2 \Omega_*/\Omega_\odot, \qquad (6)$$

is a reasonably accurate prescription at moderate rotation rates. In this expression, the mean base coronal field strength for the present day sun is denoted by $B_\odot$ (herein assumed to have the value $\sim 2$ Gauss, see Appendix A). The dependence on the stellar radius ensures the conservation of magnetic flux at a constant rotation rate. Depending on where in the stellar interior the dynamo regeneration of the field is believed to occur, one can use either the core rotation rate $\Omega_{core}$ or the rotation rate of the convection zone $\Omega_{conv}$ for $\Omega_*$. The former prescription implicitly assumes a dynamo located beneath the core-envelope boundary (in the overshoot layer), while the latter prescription assumes that the dynamo is distributed throughout the whole convection zone. At fast rotation, we consider two illustrative scenarios: 1) the mean field continues to increase linearly with rotation ; and 2) the field strength saturates at a certain rotation rate, such that $B_* = Q_{sat} \times B_\odot$ when $\Omega_* \geq Q_{sat} \times \Omega_\odot$. In panel (A), we show the evolution of the rotation rate of the core and the envelope for a solar mass star, with an initial $V_{eq} = 15$ kms$^{-1}$, using various dynamo prescriptions. The coupling time $\tau_c = 20$ Myr is taken to agree with the canonical age difference between $\alpha$ Persei and the Pleiades. We altered the linear dynamo prescription (solid line) to a saturated dynamo, in which the mean coronal field saturates when the star rotates faster than, respectively, 5 (dashed line, $Q_{sat} = 5$) and 10 (dash-dotted line, $Q_{sat} = 10$) times the present solar rotation rate. Arguments for dynamo saturation are derived from observations of coronal X-ray emission saturation among late-type stars in the Pleiades cluster (Stauffer et al. 1994; see also Vilhu 1984; Skumanich & MacGregor 1986 for results concerning chromosphere and transition region emission). The assumed parametric prescriptions and adopted parameter values are chosen to best illustrate the effect such dynamo saturation would have on the rotational history of a star. It is easily seen that dynamo saturation reduces the angular momentum loss from the stellar wind since a lower magnetic field strength at the base of the corona causes less efficient magneto-centrifugal acceleration of the plasma. The angular momentum carried away by the wind (by advection and magnetic stresses) hence is reduced. This effectively ties the core and envelope since the coupling mechanisms have sufficient time to balance the angular momentum loss from the weaker stellar wind, so that higher rotational velocities are obtained for lower field strengths (saturation at 10 versus 5 times the present solar rotation rate). The higher rotational velocities are sustained for a considerably longer timespan.

In Panel (B), we varied the coupling time ($\tau_c$), while retaining the linear dynamo prescription for the stellar wind. When the stellar wind starts to decelerate the outer convection zone, the coupling term, proportional to $(\Omega_{core} - \Omega_{conv})$, causes angular momentum to be transported from the rapidly rotating core to the more slowly rotating envelope. Stronger coupling between the two regions (shorter coupling timescale) on the PMS leads

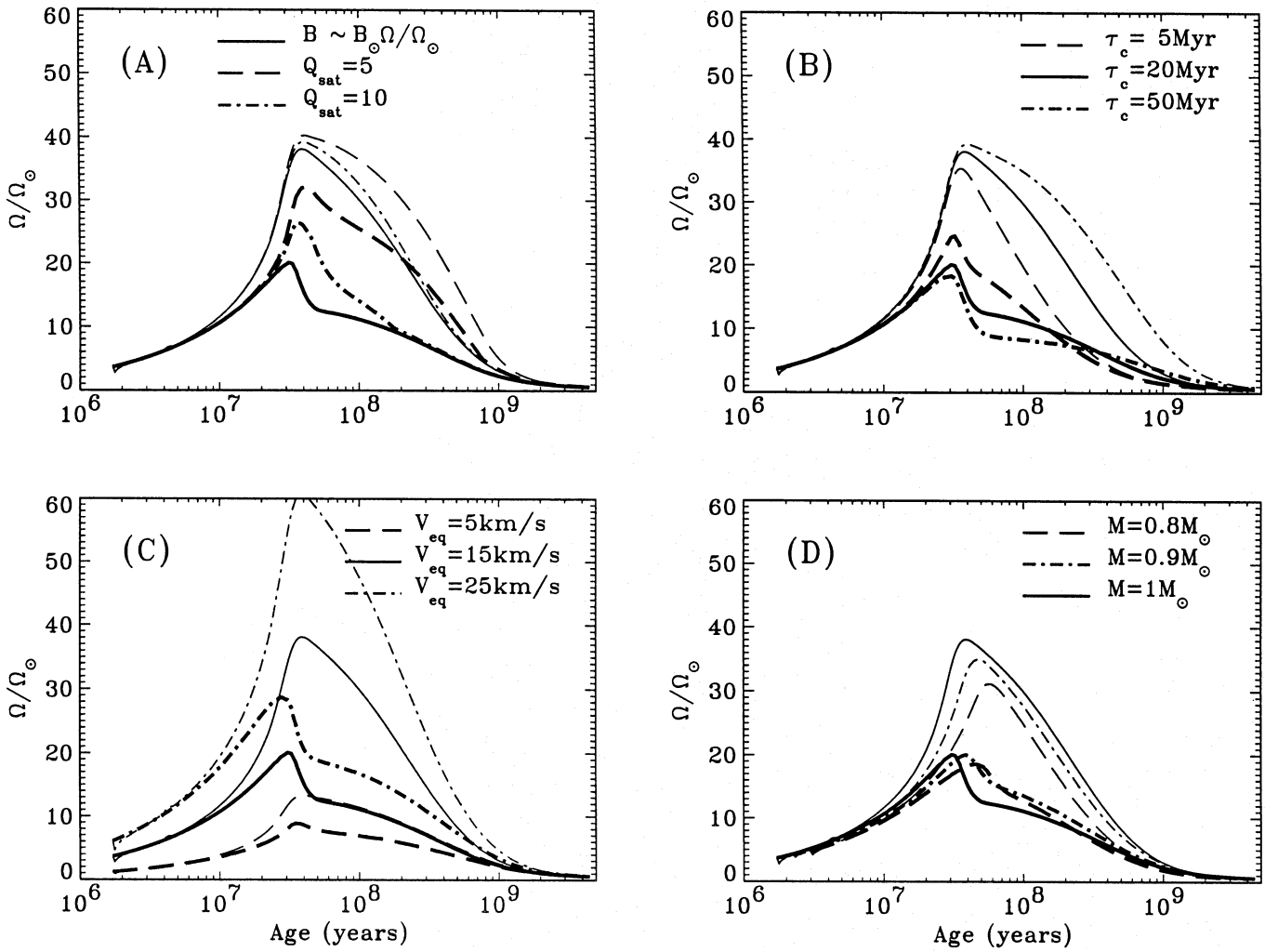


**Fig. 3a–d.** The evolution of the rotation rate (in units of $\Omega_\odot = 3 \times 10^{-6} s^{-1}$) of the core, $\Omega_{core}$, and the convective envelope, $\Omega_{conv}$ (thicker lines), for a single star. Panel **a**: for a $1M_\odot$ star, with initial equatorial velocity $V_{eq}(t_{RC}) = 15$ kms$^{-1}$, and coupling timescale $\tau_c = 20$ Myr, for three different dynamo prescriptions. The solid lines are for a linear dynamo, $B/B_\odot \sim \Omega_{conv}/\Omega_\odot$; the dashed lines for a dynamo saturated at $\Omega_{conv} \geq 5\Omega_\odot$; and the dash-dotted line for a dynamo saturated at $\Omega_{conv} \geq 10\Omega_\odot$. Panel **b**: The rotational histories for a $1M_\odot$ star, having $V_{eq}(t_{RC}) = 15$ kms$^{-1}$, and $B \propto \Omega_{conv}$ for $\tau_c = 5$ Myr (dashed line), 20 Myr (solid line), and 50 Myr (dash-dotted line). Panel **c**: a $1M_\odot$ star, with $\tau_c = 20$ Myr and a linear dynamo, for $V_{eq}(t_{RC}) = 5$ kms$^{-1}$ (dashed line), $V_{eq}(t_{RC}) = 15$ kms$^{-1}$ (solid line), and $V_{eq}(t_{RC}) = 25$ kms$^{-1}$ (dash-dotted line). Panel **d**: for a star of mass $0.8M_\odot$ (dashed line), $0.9M_\odot$ (dash-dotted line) and $1M_\odot$ (solid line), with $\tau_c = 20$ Myr, a linear dynamo, and $V_{eq}(t_{RC}) = 15$ kms$^{-1}$

to faster surface rotation rates in the late-PMS/early-MS evolution. Note how a fast convection zone spin-down occurs for a time about equal to $\tau_c$, and that 50 % spin-down can easily be achieved within this timescale. The angular momentum transported from the core to the envelope eventually forces the rotation rate of the outer convection zone to change at a rate set by the torque associated with the stellar wind, acting on the whole star, since $\tau_w$ will exceed $\tau_c$ at slower rotation rates, and both regions are effectively braked.

Panel (C) shows the influence of a higher initial angular momentum, or a difference in initial rotational velocity. Faster rotators spin up to higher rotation rates, with considerable differential rotation as a consequence of the immediate effect of the stellar wind when a faster surface rotation causes a more rapid spin-down of the convection zone to occur.

Finally, as is apparent from Panel d and Fig. 2, the rotational evolution of stars of lower mass is influenced by the different rates at which their structural evolution proceeds. Less massive stars develop their radiative core later in the evolution, and have a correspondingly lower angular momentum content. This immediately translates to a slower rotational evolution, with a spin-up to somewhat lower rotation rates for both core and convective envelope.

In the following section, we will use this parametric model for the rotational evolution of a single star to calculate the evolution of the period distribution of a star cluster.

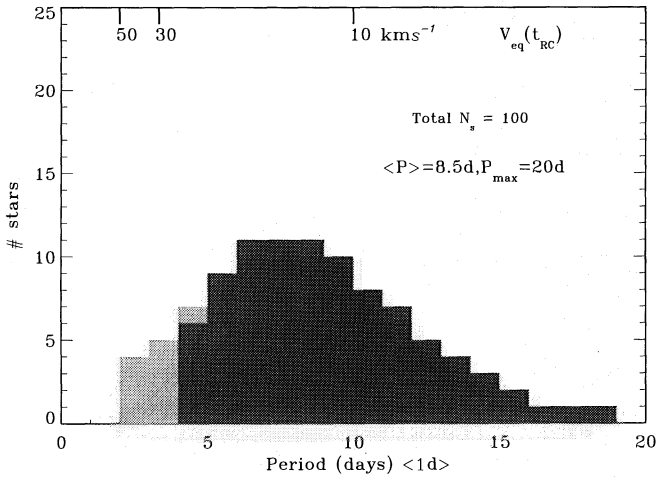


**Fig. 4.** The initial Maxwellian period distribution, with the longest period $P_{max}$ = 20 days, and a mean period $< P >$= 8.5 days. The total number of stars in the distribution is $N_s$ = 100, and the corresponding equatorial velocities range up to 50 kms$^{-1}$. The velocity scale (top axis) gives the equatorial velocity for a solar mass star at about 1.7 Myr. 90 stars (darker shaded) rotate slower than 25 kms$^{-1}$

## 3. Evolution of stellar distributions

To calculate the evolution of a period distribution, we proceed as follows. We determine the rotational evolution for sets of single stars with identical mass, dynamo prescription, and coupling timescale, with inital equatorial velocities $V_{eq}(t_{RC}) \in [5, 10, 15, 20, 25, 30, 35, 40, 45, 50]$ (in kms$^{-1}$). A prescribed initial period distribution is then converted to a distribution of equatorial rotational velocities at $t_{RC}$, and the linear interpolation of this distribution within the set $[5, 10, 15, 20, 25, 30, 35, 40, 45, 50]$ at $t_{RC}$ is subsequently evolved in time, pulling this interpolated distribution through the calculated $\Omega(t)$-tracks. The distribution of the rotation rates at a certain time is then recovered by converting the evolved distribution at that age in a histogram with a given bin width (we use bins of width $3 \times \Omega_\odot$ throughout).

The assumed initial distribution will naturally influence the evolutionary picture we obtain from evolving each star in the distribution according to Eqs. (1)-(2). In particular, we introduce a range in periods and a mean rotation period, which are both important restricting parameters for the angular momentum distribution. We consider how an initial Maxwellian distribution of periods for TTS (Fig. 4) evolves. This distribution for period $P$ (in days) is given by

$$f(P) = AP^2 \exp(-\frac{4}{\pi}(\frac{P}{< P >})^2), \quad (7)$$

where $A$ is a normalization constant, and $< P >$ is the mean rotation period. We ignore the possibility of an intrinsic age spread in the cluster, although such spreads may well occur and alter the rotational evolution of the period distribution. We choose a mean rotation period $< P >$= 8.5 days and a range of periods up to 20 days for the initial Maxwellian[4]. The mean period of 8.5 days is taken in accord with the observed mean rotation period for the slowly rotating CTTS (Attridge & Herbst 1992). We therefore have fewer rapidly rotating stars at the T Tauri age than the observed bimodal (slowly rotating CTTS/rapidly rotating WTTS) period distribution of TT stars. This limits the range in angular velocity found at later times. The Maxwellian period distribution corresponds to initial equatorial velocities up to a maximum value of 50 kms$^{-1}$, with most (90 %, darker shade in Fig. 4) TT stars rotating slower than 25 kms$^{-1}$. Taking the maximal period equal to 20 days sets the longest rotation period in the histogram at about 18 days. This is in agreement with the longest rotation period found by Attridge & Herbst (1992), namely 17.25 days. The longest rotation period found by Bouvier et al. (1993) was 12 days, while they were able to observe periods of up to 30 days. It thus seems suitable to introduce a slow rotational velocity cut-off (maximal period $P_{max}$). In the following discussion, we limit ourselves to this initial period distribution; the interpretation of the results, as well as any comparison with observed rotational velocities (Fig. 1) must take this assumption into account.

### *3.1. Linear and saturated dynamos*

We first consider how the dynamo prescription influences the evolution of the stellar rotational velocity distribution. The dynamo law enters the evolutionary calculation (Eqs. (1)-(2)) through the spin-down timescale $\tau_w$, which is updated at each timestep using the WD model for the stellar wind (see Appendix A). As was shown in Fig. 3a, when the dynamo field saturates (we took $Q_{sat}$ = 5, 10), the weaker (compared to the linear dynamo case) field causes a slower spin-down (longer $\tau_w$), and the core and the envelope are more effectively coupled. Therefore, higher surface rotation rates are achieved and sustained for a longer time.

In Fig. 5, we show how the initial Maxwellian period distribution (Fig. 4) evolves in time under three different dynamo prescriptions. We assume that all stars have $M_* = M_\odot$, and that the core-envelope coupling mechanisms act on a typical timescale $\tau_c$ = 20 Myr. We choose four representative ages in the evolution. The first timeframe corresponds to a late PMS age of 30 Myr, at which time the surface rotation of a typical $1M_\odot$ star reaches its maximum (see Fig. 3). Other timeframes correspond to the canonical ages of the $\alpha$ Persei, the Pleiades and the Hyades cluster, respectively, and should be compared with the observed $v \sin i$ distributions shown in Fig. 1. It is obvious from the single star calculations shown in Fig. 3 that the initial Maxwellian evolves smoothly into the distribution shown at $t$ = 30 Myr, with each star spinning up to a rate proportional to its initial angular velocity. Such a homologous evolution is expected in the absence of angular momentum loss. Beyond about 30 Myr the timescale characterizing internal, structural

[4] The Maxwellian distribution for the periods was discretized to a histogram by integrating over bins with a one day width. The distribution was then renormalized using the maximal period $P_{max}$ = 20 days.

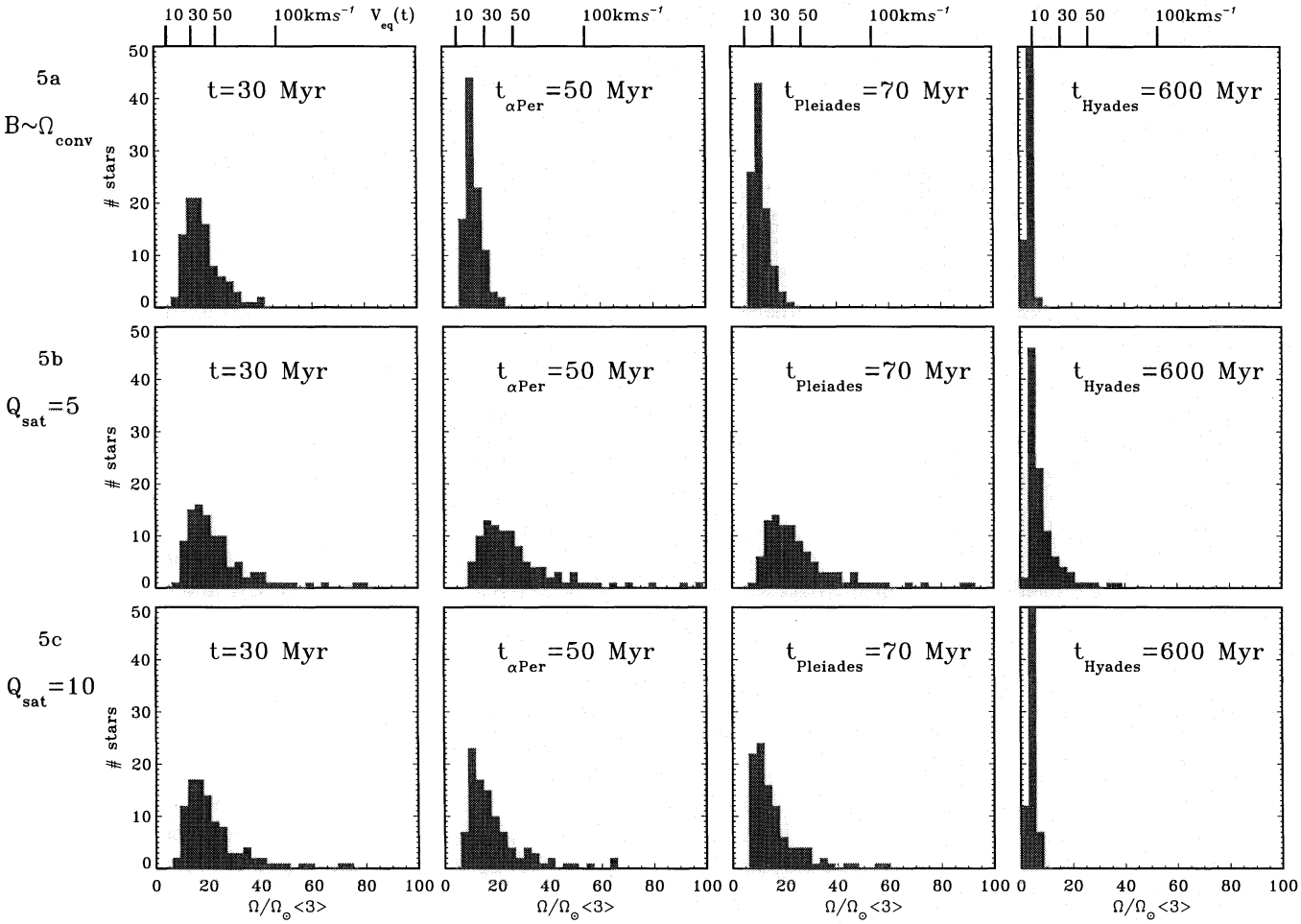


**Fig. 5a–c.** The evolution of the initial Maxwellian period distribution of Fig. 4, when all the stars in the distribution are of solar mass and have $\tau_c$ = 20 Myr. Shown are the distributions of the rotation rate $\Omega_{conv}$ (bins are of width $< 3\Omega_\odot >$) at 4 representative ages: 30 Myr (left), 50 Myr (age of $\alpha$ Persei), 70 Myr (age of the Pleiades), and 600 Myr (right, Hyades age). Top **a**: evolution under a linear dynamo law $B \sim \Omega_{conv}$. Middle **b**: evolution under a saturated dynamo ($Q_{sat}$ = 5). Bottom **c**: as **b**, for $Q_{sat}$ = 10. Corresponding equatorial velocities are shown on top for a solar mass star at that age

changes becomes longer than $\tau_w$, and the action of the stellar wind dominates the rotational evolution. At later times ($t \geq 600$ Myr), all stars in the distribution are slowly rotating, attaining a surface rotation rate $\approx \Omega_\odot$ at the solar age.

In Fig. 5a, the Maxwellian (corresponding to initial equatorial velocities ranging up to 50 kms$^{-1}$) evolves under a *linear dynamo* prescription (Eq. (6)), with the mean base coronal field proportional to the envelope rotation rate $\Omega_{conv}$. At 30 Myr, rotation rates range from 8 to 40 times solar, with roughly 80 % of all stars rotating with $V_{eq} \leq 50$ kms$^{-1}$ and 30 % rotating slower than 30 kms$^{-1}$. At 50 Myr (the age of the $\alpha$ Persei cluster), the fast spin-down of the stellar envelope within a time of order $\tau_c$ = 20 Myr, results in a shift of the whole rotational distribution to velocities below 40 kms$^{-1}$, with about 90 % of the stars rotating slower than 30 kms$^{-1}$. The maximal rotational velocity is reduced from 86 kms$^{-1}$ at 30 Myr to 41 kms$^{-1}$ at 50 Myr. The linear dynamo prescription thus seems consistent with a 50 % spin-down of the envelope within 20 Myr, but this spin-down occurs too early in the rotational evolution. After this dramatic spin-down, the distribution evolves continuously into a $\delta$-type distribution at the Hyades age, with essentially all stars rotating slower than 10 kms$^{-1}$. We note however that, at the age of the Pleiades (70 Myr), the distribution is virtually identical to the rotational distribution at 50 Myr, and that all stars still rotate faster than the 10 kms$^{-1}$ threshold. This is because, after the initial fast spin-down of the envelope, the decreased surface rotation rate leads to less effective braking by the stellar wind, and the braking timescale $\tau_w$ becomes longer than the coupling timescale $\tau_c$. Thus, the wind effectively has to brake down the whole star, and due to the star's large moment of inertia, the rotation rate decreases very gradually.

In Fig. 5b, we present the rotational evolution for a *saturated dynamo* ($Q_{sat}$ = 5). At 30 Myr, we recover a range of stellar rotation rates from 8 to 80 (!) times the present solar rotation rate (when only stars initially rotating at less than 25 kms$^{-1}$ are taken into account - 90 % of the initial Maxwellian - we recover a range in stellar rotation rates identical to the linear dynamo prescription: 8 to 40 times $\Omega_\odot$). At this time, about 60 % of

all stars rotate slower than 50 kms$^{-1}$, and 20 % slower than 30 kms$^{-1}$. Through the more effective core-envelope coupling that results from a weaker stellar wind (weaker magnetic field), the envelope gains more angular momentum from the faster rotating core (through the coupling term $\Delta J/\tau_c$) and therefore, the initial distribution (with $V_{eq} \leq 50$ kms$^{-1}$) evolves into a broad distribution of rotation rates, with a maximal rotational velocity of about 170 kms$^{-1}$ at 30 Myr. At the age of $\alpha$ Persei, a slight spin-up extends the range up to roughly 97 $\Omega_\odot$ (the initial maximal $\Omega_{max} = 11.5\Omega_\odot$). However, only 20 % of all stars rotate slower than 30 kms$^{-1}$. At 70 Myr, the gradual spin-down has influenced the distribution only slightly (the fastest rotator spun down by 10 kms$^{-1}$, while the slowest spun down by 2 kms$^{-1}$), and even at the Hyades age, about half (50 to 60 %) of the stars still rotate faster than 10 kms$^{-1}$. In summary, this dynamo saturation ($Q_{sat} = 5$) causes a large spread in the rotational distribution at the correct age (50 Myr), but fails to reproduce the spin-down that should occur at later times.

In Fig. 5c, we show that dynamo saturation at a higher rotation rate ($Q_{sat} = 10$) combines some of the features of the previous dynamo prescriptions. While the desired spread in rotation rates still occurs, more stars end up rotating slower than 30 kms$^{-1}$ (70 %) at 70 Myr, and at the Hyades age of 600 Myr, almost none (5-10 %) rotate faster than 10 kms$^{-1}$ (maximal rotational velocity is 16.5 kms$^{-1}$). However, there are still rather few slow rotators ($V_{eq} \leq 10$ kms$^{-1}$) at the Pleiades age.

To account for slow rotators at the Pleiades age (50 % rotating slower than 10 kms$^{-1}$, see Fig. 1), one needs a more effective spin-down of the stellar envelope. Since the single star calculations described in Sect. 2 indicate that the stellar cores rotate faster than the stellar envelopes at the ages considered (see Fig. 3), a dynamo law which links the mean coronal field to the core rotation rate will cause more rapid spin-down (shorter $\tau_w$) through the action of a stronger stellar wind. We have calculated (not shown in Fig. 5) how extremely effective this spin-down mechanism is, by evolving the initial distribution under a linear dynamo law in which the field is proportional to the core rotation rate $\Omega_{core}$. All stars in the distribution end up rotating slower than 10 kms$^{-1}$ at 50 Myr. In fact, the fastest rotator at 30 Myr becomes the slowest at 50 Myr, and from about this age on, the coupling term ($\Delta J/\tau_c$) acts as a source term for the angular momentum of the envelope, causing a slight spin-up of the surface layers in the later evolution, but the rotational velocities stay within the narrow range [0-10 kms$^{-1}$] from 50 Myrs on. We refer to Soderblom et al. (1993) for a calculation of the rotational evolution of a distribution of rotational velocities when the dynamo field depending on the core rotation rate saturates at fast rotation.

The results of this section can be summarized as follows: a linear dynamo produces adequate spin-down early in the evolution but fails to produce sufficiently rapid rotators at the ages of $\alpha$ Persei and the Pleiades; a saturated dynamo can explain the observed large spreads in rotation rates but the level of saturation is constrained by the requirement of achieving spin-down to slow rotation by the Hyades age; a submerged linear dynamo ($B_* \sim \Omega_{core}$) causes effective spin-down to slow rotation rates. Clearly, dynamo-related effects are important, but must be complemented by other physical mechanisms in order to explain all characteristics of the observed scenario for angular momentum evolution.

### 3.2. Coupling mechanisms

As the effects described in the previous section are quite naturally explained in terms of the two timescales dominating the rotational evolution after the initial spin-up phase ($\tau_c$ and $\tau_w$), one can expect that, for a given dynamo prescription ($\tau_w$), similar effects can be modelled by changing the coupling timescale $\tau_c$. In Fig. 6, we compare the rotational evolution of solar mass stars with their field strengths linked to the star's rotation rate by a saturated dynamo ($Q_{sat} = 10$), for a coupling timescale of 5 Myr (Fig. 6a), 20 Myr (Fig. 6b=Fig. 5c) and 50 Myr (Fig. 6c).

For an initial range of equatorial velocities up to 50 kms$^{-1}$, the spread in rotation rates reaches a maximum value 87 $\Omega_\odot$ for $\tau_c = 5$ Myr, 73 $\Omega_\odot$ for $\tau_c = 20$ Myr and 67 $\Omega_\odot$ for $\tau_c = 50$ Myr. The coupling timescale, by definition, regulates the angular momentum transport from the core to the envelope and is therefore an immediate measure of the spread in rotational velocity that can be achieved from a given initial range in the period distribution. A shorter coupling timescale causes a faster exchange of angular momentum at the core-envelope boundary, and thus a faster surface rotation. For the saturated dynamo law considered ($Q_{sat} = 10$), this effect is most prominent at about 50 Myr, with equatorial velocities up to 160 kms$^{-1}$, 120 kms$^{-1}$ and 95 kms$^{-1}$ for a coupling timescale of 5 Myr, 20 Myr and 50 Myr, respectively. The subsequent gradual spin-down of the star proceeds almost independent of $\tau_c$, since, as soon as the spin-down timescale $\tau_w$ is comparable to or longer than the coupling timescale $\tau_c$, the stellar wind has to brake the whole star (as opposed to only the envelope), a process which depends on the moment of inertia of the entire star, rather than on the actual coupling timescale $\tau_c$ itself.

### 3.3. Stellar mass

In the cases presented so far, all stars in the distribution were assumed to have a mass equal to that of the sun (1M$_\odot$). However, the observed $v \sin i$ distributions as shown in Fig. 1, cover a range in stellar mass from about 0.8M$_\odot$ to 1M$_\odot$. Since stars of smaller mass have a somewhat slower (with respect to 1M$_\odot$ stars) rotational evolution (see Fig. 3), a different structural evolution (Fig. 2), and a smaller initial angular momentum content, we expect those stars to rotate somewhat slower than more massive stars. This effect is illustrated in Fig. 7, where we compare how the initial Maxwellian with a saturated dynamo prescription ($Q_{sat} = 5$) evolves when all stars are of mass 0.8M$_\odot$ (Fig. 7a), as opposed to 1M$_\odot$ (Fig. 7b = Fig. 5b). For stars of mass 0.8 M$_\odot$, the minimal ZAMS radius is reached at 82 Myr (Fig. 2), and we note that these stars are still spinning up at 30 and 50 Myr, with their maximum rotation rates attained at roughly the age of the Pleiades, for the saturated dynamo prescription

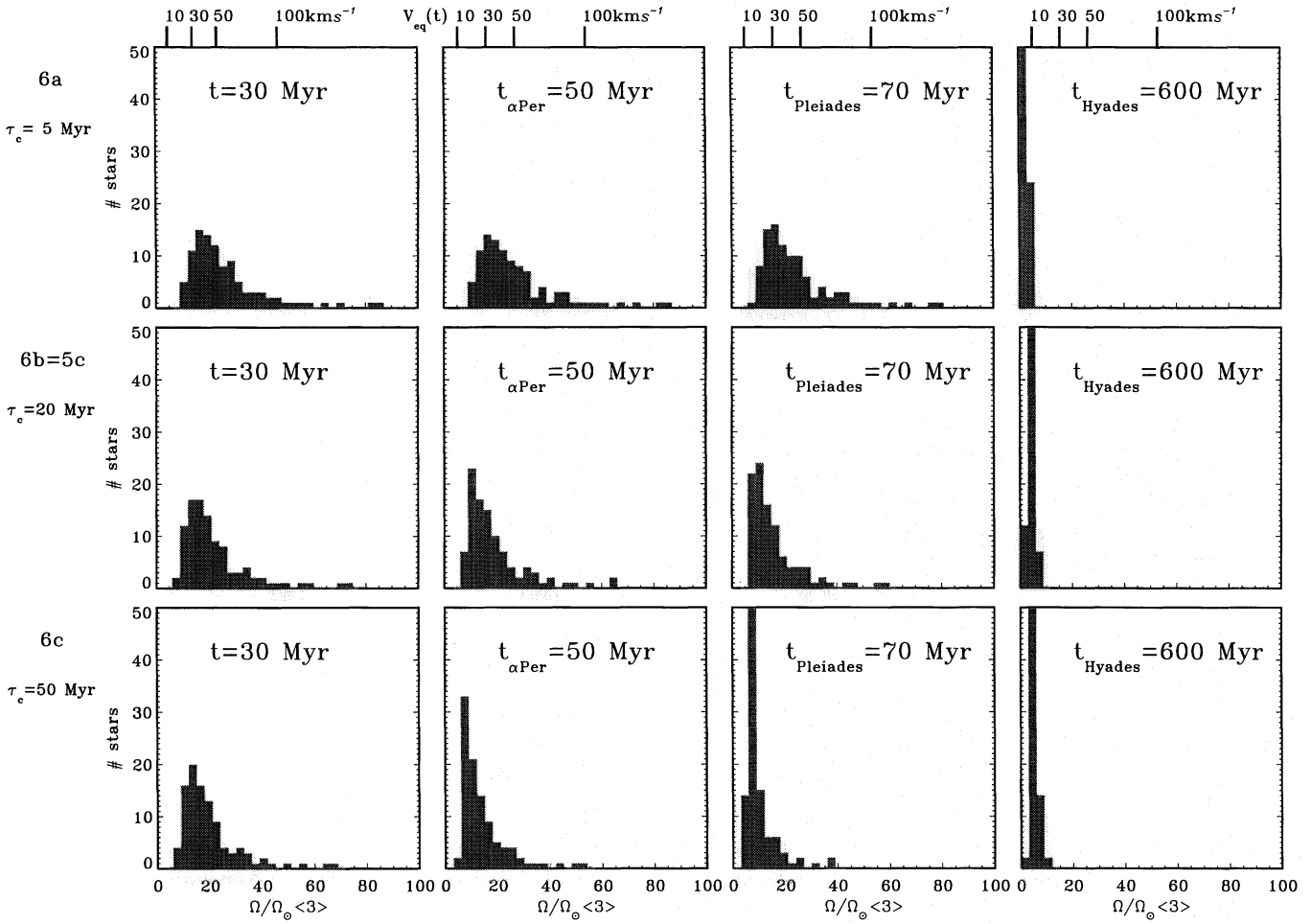


**Fig. 6a–c.** In the same format as Fig. 5, the evolution of stars with $M_* = M_\odot$ and a saturated dynamo with $Q_{sat} = 10$. Top **a**: for a coupling timescale $\tau_c = 5$ Myr. Middle **b**: $\tau_c = 20$ Myr (as in Fig. 5c). Bottom **c**: $\tau_c = 50$ Myr

invoked. Even though this particular dynamo relation fails to reproduce the low rotational velocities observed at the Hyades age for $1M_\odot$ stars (Fig. 7b, with velocities up to 70 kms$^{-1}$), for the same dynamo, 90 % of all $0.8M_\odot$ stars do end up rotating slower than 10 kms$^{-1}$ at 600 Myr (maximal rotational velocity of 27 kms$^{-1}$). This suggests that the presence of a significant fraction of late G-early K stars in the distribution (or 0.8-0.9 $M_\odot$ stars) may account for part of the observed population of slow rotators. Observational support for this hypothesis remains, at this juncture, inconclusive. Plots of measured $v \sin i$ values as a function of the color index $B - V$ for both $\alpha$ Persei (Fig. 17 in Prosser 1992) and the Pleiades (Fig. 8 in Soderblom et al. 1993) do not show any obvious difference in rotation rates between stars of different colors ($B - V$ in [0.55-0.85]). The discrepancy may result either from difficulties that arise in converting an observed color index to a true mass range (corrections must be made to the observed colors due to reddening, stellar metallicity,...), or may tell us something about differential star formation in clusters, since in our model calculations, all stars are 'formed' at the same age, regardless of their final total mass.

### *3.4. Disk-regulating mechanisms*

Although, as noted earlier, the initial Maxwellian distribution for the rotation periods of TTS was chosen to have more slow rotators than actually observed, the predicted evolution of the period distribution was unable to account for the large fraction of slow rotators (2/3 rotating slower than 30 kms$^{-1}$ for the $\alpha$ Persei cluster, and 50 % rotating slower than 10 kms$^{-1}$ for the Pleiades) found in young clusters. One possible solution to this problem is to invoke a dynamo law in which the magnetic field depends on the core rotation rate, causing a faster spin-down to occur (see discussion of Sect. 3.1). This may well be true for some stars in the initial distribution, but cannot be true for all stars, since this dynamo prescription fails to yield the observed large spread in rotation rates, unless this dynamo law is saturated. In this section, we will consider an alternative scenario, wherein part of the initial distribution of stars has its rotation rate regulated by disk accretion and disk-star magnetic coupling. In particular, we compare the evolution of the period distribution when a certain fraction of the initial Maxwellian keeps rotating with constant period for a prescribed time $\tau_D$ beyond the formation of the radiative core at $t_{RC}$. Since before this time, the same physical

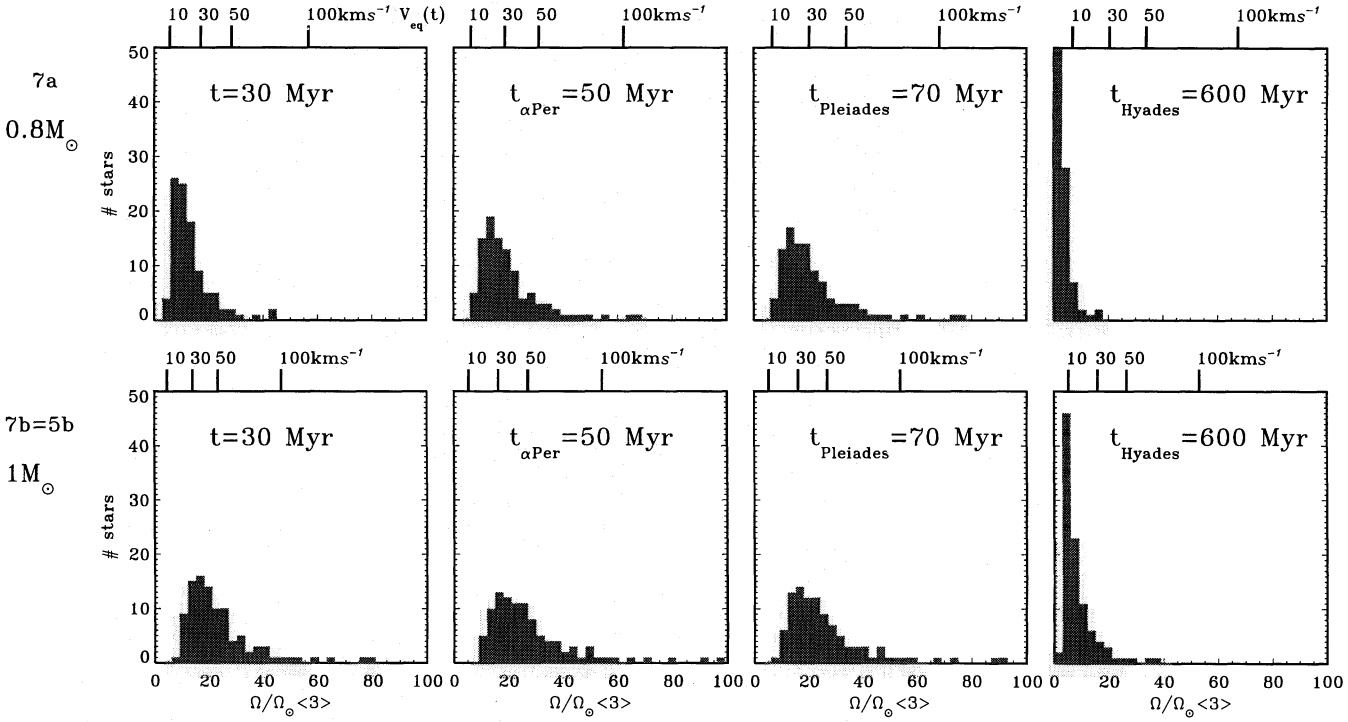


**Fig. 7a and b.** As in Figs. 5and 6: the rotational evolution for a saturated dynamo ($Q_{sat}$ = 5) with $\tau_c$ = 20 Myr. Top **a**: all stars have stellar mass 0.8M$_\odot$. Bottom **b**: all stars have mass 1M$_\odot$ (identical to Fig. 5b). Note the range in rotation rates and the different equatorial velocity axis for 0.8 versus 1 solar mass stars of a given age

processes have been operative, we will assume that the fraction $f_D$ of the initial distribution possessing disks, coincides with the $f_D N_s$ slowest rotators in the distribution (of $N_s$ stars). In this way, we recover in some very approximate way, the observed bimodal period distribution of the TT stars.

In Fig. 8, we present some typical cases, where the initial Maxwellian distribution (with $V_{eq}$ ranging up to 50 kms$^{-1}$) for solar mass stars evolves under a linear dynamo law ($B_* \sim \Omega_{conv}$). Figure 8 should be compared to Fig. 5a, which shows the evolution for stars without disks. In Fig. 8a, one-fourth of the initial distribution (the 25 slowest rotators from Fig. 4), has a disk for 3 Myr beyond $t_{RC}$. These stars never reach rotational velocities exceeding 20 kms$^{-1}$, throughout their entire evolution. When we take a larger fraction of the initial distribution ($f_D$ = 1/2, $\tau_D$ = 3 Myr, Fig. 8b), more stars accumulate at the low rotational velocity end of the distribution. A large population of slow rotators at the ages of $\alpha$ Persei and the Pleiades can be produced upon (artificially) assuming that half the stars have a disk for 10 Myr beyond $t_{RC}$ (cf. Fig. 8c).

More realistically, one needs to account for a distribution of disk timescales $\tau_D$ among the fraction $f_D$. Additionally, since we choose this fraction to coincide with the initial slowest rotators, we, in effect, maximize the number of slow rotators produced by the disk regulating mechanism. We have looked at cases in which the slow rotators are randomly distributed throughout the initial Maxwellian, and a net increase in slower rotators does remain present in the later evolution, although to a somewhat lesser extent than in the results under consideration. However, it is evident that a more accurate description of disk regulation is necessary (see also Appendix B). The calculations presented in Fig. 8 merely serve to illustrate how such a mechanism can potentially account for the large fraction of slow rotators observed in both $\alpha$ Persei and the Pleiades.

### *3.5. Comparison with recent model calculations*

In this section, we compare our results with some of the recent model calculations on rotational evolution of stellar distributions. Soderblom et al. (1993) performed a similar calculation of the evolution of a distribution of rotational velocities. While they used the same model (Eqs.. (1)-(2)) to calculate the angular momentum evolution, our calculations differ in the use of updated evolutionary tracks and WD wind solutions, and, in particular, the consistent incorporation of gravitational effects (Appendix A). Their result was obtained for a saturated dynamo (with the saturation tied to the core rotation) with a high critical rotation rate ($Q_{sat}$ = 40), and was naturally influenced by the initial distribution for the rotational velocities (Maxwellian and lognormal). The adopted coupling timescale was 20 Myr. The present calculations, confirm the qualitative agreement with observed rotational velocities that was obtained, and show how this agreement can be improved upon when considering other physical parameters that may play a role in the suggested scenario for the evolution of rotational velocities.

We argue that effective coupling between the core and the envelope can explain the observed spread in rotational veloc-

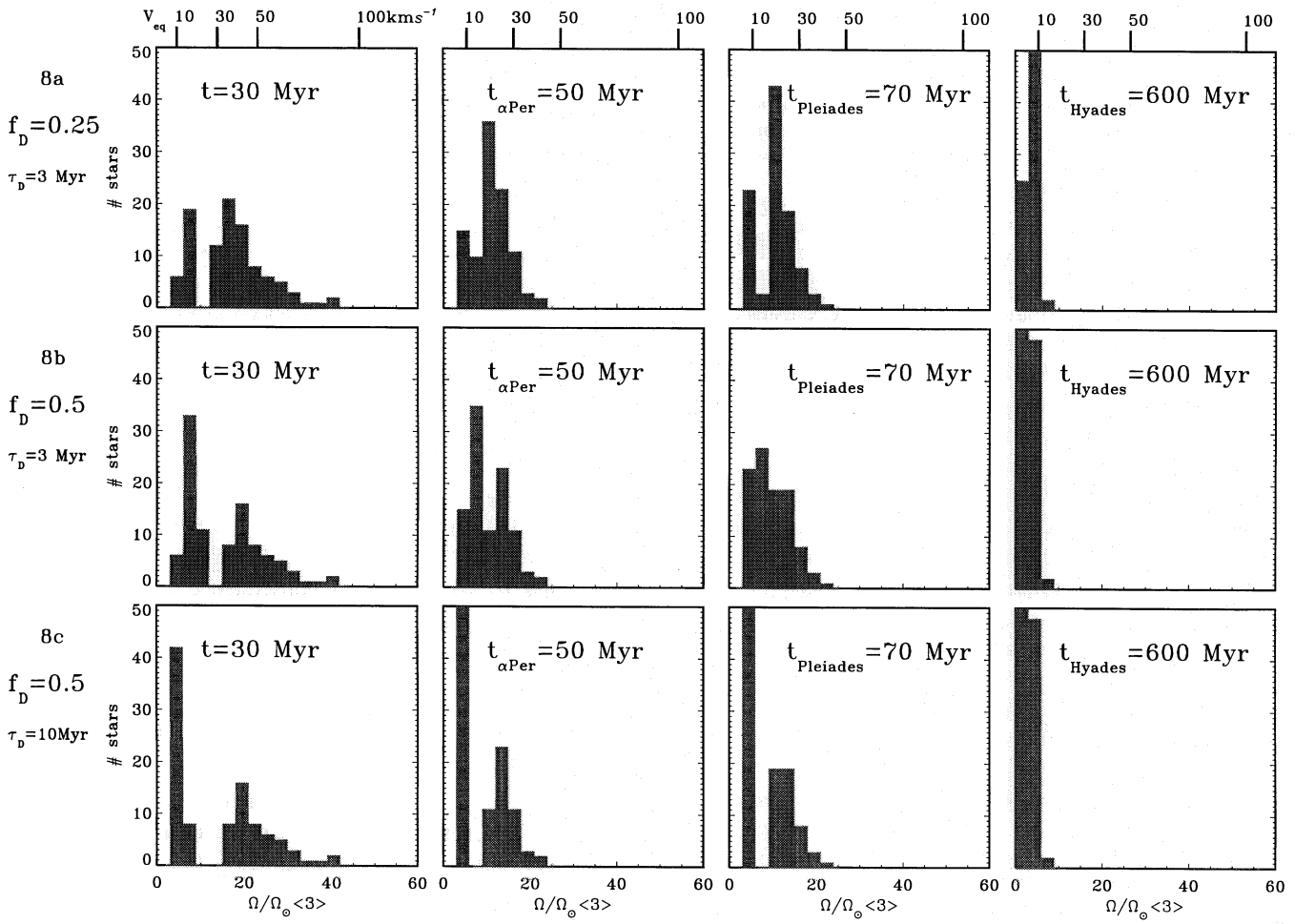


**Fig. 8a–c.** The evolution of the initial Maxwellian ($N_s$ = 100) under a linear dynamo law ($B \sim \Omega_{conv}$) for solar mass stars with $\tau_c$ = 20 Myr. Top **a**: when the 25 slowest rotators in the initial Maxwellian have a disk (constant rotation period) for 3 Myr past $t_{RC}$. Middle **b**: when the 50 slowest rotators in the Maxwellian have a disk for 3 Myr beyond $t_{RC}$. Bottom **c**: when the slower half of the initial distribution has a disk for 10 Myr beyond $t_{RC}$. Compare with Fig. 5a, note the change in the range of rotation rates

ity. It is therefore evident that in the limit of no differential rotation ($\tau_c \rightarrow 0$), extremely high rotational velocities can be obtained, as Bouvier (1994) has pointed out. However, the rotational evolution of rigidly rotating stars, as described by Bouvier (1994) is unlikely because of the unphysical nature of his assumed braking law. Bouvier calculated the evolution of surface rotation under solid-body rotation, disk-locking of the rotation rate for prescribed disk ages ranging from 0.7 to 50 Myr, and a parametric wind braking law, using PMS evolutionary models and representative MS stellar parameters. His adopted braking timescales ($\equiv V_{eq}/(dV_{eq}/dt)$), as based on the parametric description of Kawaler (1988), are derived from the braking laws

$$\frac{dV_{eq}}{dt} \propto K_{slow} V_{eq}^3 \quad for \quad V_{eq} < V_{crit}$$
$$\frac{dV_{eq}}{dt} \propto K_{fast} V_{eq}^2 \quad for \quad V_{eq} > V_{crit},$$

and are artificially prolonged by a factor of 10 (resulting from the discontinuous change in the free parameter $K_{slow}$ to $K_{fast}$ = $8.33 K_{slow}$) when a critical equatorial velocity of $V_{crit}$ =60 kms$^{-1}$ is exceeded. Thus, even though magnetic braking is assumed to operate during both PMS and MS evolution, the rigidly rotating stars can spin up to extremely high rotation rates ($V_{eq}$ up to 180 kms$^{-1}$) throughout the course of PMS contraction, since the presumed braking timescale is *longer* for faster rotation. This is quite opposite to the true shortening of $\tau_w$ when the rotation rate increases, and the resulting spin-down of the outer envelope in the late PMS stages (see Fig. 3, Fig. 5a). After this dramatic spin-up, the rigidly rotating stars are subsequently spun down in a very short time (see Bouvier 1994, his Fig. 2). This is a consequence of the large stellar wind torque applied to the star, which is overestimated by the Kawaler expressions. Indeed, the magnitude of the torque implied by the parametric formulae for a solar-type star rotating at 60 kms$^{-1}$ is of the order of $10^{35}$ dyne cm when taken as a slow rotator ($V_{eq} \leq V_{crit}$ = 60 kms$^{-1}$). The WD estimate yields a torque at such rotation rates of order $10^{34}$ dyne cm (see Fig. 10, Appendix A). Since the torque as calculated from a WD model with similar coronal conditions, is known to overestimate the true torque applied, for a more realistic axisymmetric base field configuration, the

torque in the Bouvier model is *at least* a factor of 10 too large. This is the case even though one parameter was chosen such that a partly closed magnetic field configuration was adopted. Since $I_*/I_{conv} \sim 10$, and in reality, the wind-induced torque is applied directly to the surface layers, taking the torque proportional to the moment of inertia of the convection zone would qualitatively resolve this unphysical prescription.

Additionally, the proposed effective coupling is quite opposite to the suggested weak coupling model (long timescale $\tau_c$), advanced by Li & Collier Cameron (1993). These authors evolved the velocity distribution of the $\alpha$ Persei cluster using a similar two-component model (rigidly rotating core and envelope), where the wind-induced torque $\dot{J}$ was taken proportional to $\Omega^3$ up to a critical rotation, and proportional to $\Omega$ for faster rotation, to account for dynamo saturation. While, at moderate ($\Omega \sim \Omega_\odot$) and high ($\Omega > 30\Omega_\odot$) rotation, these parametric prescriptions are in reasonable accord with the WD prescription we adopted (see Appendix A, Fig. 10), there is a clear discrepancy for intermediate rotation (note however that, as long as the applied braking torque is lower than the WD prescription which may overestimate the torque, one cannot dismiss any inferred discrepancy). Furthermore, the stars in the adopted initial $\alpha$ Persei distribution had identical rotation rates for core and envelope, while our calculations indicate that the differential rotation achieved during the PMS contraction phase is quite crucial at about this age. Because of this initial solid-body rotation, weak coupling (long $\tau_c$) was able to recover the spin down from an adopted maximum rotational velocity of 180 kms$^{-1}$ at $\alpha$ Persei, to a maximum of 40 kms$^{-1}$ adopted for the Pleiades (compare with Fig. 1). The apparent disagreement thus arises when these authors try to fit in detail an adopted velocity distribution for the Pleiades and the Hyades, from an initial adopted distribution for the $\alpha$ Persei cluster, while we infer reasonable estimates for the model parameters from their influence on the PMS/MS evolution of an initial TTS distribution, by comparing them with the observed velocity distributions of these clusters. In particular, we found no evidence for their claim of an extremely slow rotation rate for the early sun, as all low mass stars evolved using our model end up rotating at solar-like rotation rates.

## 4. Discussion and conclusions

Within the limits of our model, we have illustrated how the important physical parameters affecting the rotational evolution of a low mass star influence the evolution of the period distribution of a cluster of such stars. The most important physical processes influencing the evolution of angular momentum for solar-type stars are the internal structural changes which occur during the approach to the MS (i.e., the development of a radiative core and the overall contraction of the star), the visco-magnetic coupling (with timescale $\tau_c$) between the core and the overlying convection zone, and the angular momentum loss associated with the stellar wind (the braking timescale $\tau_w$). During most of the PMS evolution, the changing internal structure of the star dominates other effects, and the star spins up to become a differentially rotating object. The degree of differential rotation that develops depends on the coupling timescale $\tau_c$. In the late-PMS/early-MS evolution, the rotational evolution is determined mostly by the coupling and braking timescales. We explored reasonable prescriptions for the coupling timescale, and in an effort to estimate the braking timescale in a deterministic and physically consistent way (incorporating changes in gravity, rotation and magnetic field), we have used the Weber-Davis MHD wind model (Weber & Davis 1967). Independent of its early rotational history, a low mass star ends up rotating at about the solar rotation rate at the solar age.

We have shown that the assumed phenomenological dynamo law that links the mean coronal field to the stellar rotation rate, through its impact on the braking timescale as a result of the magneto-centrifugal character (in addition to the thermal character) of the stellar wind at high rotation rates, has a definite influence on the evolution of the period distribution. A linear dynamo law, in which the field strength increases linearly with increasing rotation rate, causes the whole distribution to spin down within about a coupling timescale ($\tau_c$, taken to be a few times 10 Myr). This is a consequence of the temporary decoupling of the convective envelope from the radiative interior. However, this spin-down occurs too early in the evolution (in the late PMS), and a large spread in rotation rate at later times (as observed in $\alpha$ Persei) cannot be achieved. A saturated dynamo law, in which the field strength remains constant above a specified critical rotation rate, does allow for large spreads. Dynamo saturation reduces the angular momentum loss from the stellar wind, and higher rotational velocities are sustained for a longer time. On the other hand, the critical rotation above which saturation occurs, must be sufficiently rapid (more than 10 times the present solar rotation rate), in order that the saturated field be strong enough to produce effective spin-down to low rotation rates ($V_{eq} \leq 10$ kms$^{-1}$) by the age of the Hyades cluster. The observed large spreads in rotational velocities of near-ZAMS distributions (up to 200 kms$^{-1}$ in $\alpha$ Per) can alternatively be explained by effective coupling between the core and the envelope (short coupling timescale $\tau_c$), such that the angular momentum content of the core (which is large because of its large moment of inertia and its fast rotation) serves as a source of angular momentum for the envelope. We have shown that this coupling timescale influences the extent of the spread in rotational velocities that can be achieved when a certain dynamo law is applied for the calculation of the braking timescale, i.e. a shorter $\tau_c$ yields higher maximal rotation rates. Therefore, we could tentatively explain the observed spread in rotation rate at young MS ages by dynamo saturation and/or short coupling timescales. Apart from the observed spreads, the $v \sin i$ distributions of young open clusters also show a large number of slow rotators. We argue that the mass spread in the clusters can influence the distributions, with less massive stars rotating slower than massive ones, on average. Alternatively, when the dynamo generated field is dependent on the (fast) core rotation rate rather than on the surface rotation, stars can be found to spin down faster, and more slow rotators will be present in the early MS distributions. Of course, the possibility remains that part of the initial T Tauri distribution has intrinsically lower than

average rotation rates. The lower rotation rates for the CTTS are attributed to the presence of accretion disks, which presumably induce a torque balance along the early PMS contraction phase. This initial bimodality in the period distribution, together with the imposed artificial bimodality in disk lifetimes (some stars have no disks, while others loose their disk after a preset lifetime), can produce a large population of slow rotators at the ages of the clusters considered.

With these results at our disposal, it is tempting to use our parametric model to try and evolve the observed bimodal TTS distribution into those of the observed clusters (Fig. 1) by suitably selecting the parameters influencing the evolution of the period distribution. The result of such an exercise is shown in Fig. 9, for the following choice of parameters: (i) a coupling timescale $\tau_c = 10$ Myr; (ii) a saturated dynamo with $Q_{sat} = 20$; (iii) a circumstellar disk for stars with initial rotation period longer than 5 days, with $\tau_D = 4$ Myr; and (iv) 0.8 and 1.0 solar mass stars in equal proportion. Specifically, the assumed parameters represent one choice of physically reasonable values, in accord with order of magnitude estimates for each of the processes they parametrically express: (i) the timescale for visco-magnetic coupling between the radiative core and the convective envelope; (ii) dynamo saturation above a critical rotation rate; (iii) proportion of CTTS versus WTTS, and the lifetimes for circumstellar disks around the CTTS (e.g. Stauffer 1994); and (iv) the proportion of low versus high mass stars in a cluster. It can be seen that the resulting evolutionary scenario suggested is qualitatively consistent with the observed rotational velocity distributions for young clusters. In particular, it produces a population of slow rotators at 50 and 70 Myr, a large spread in rotational velocity at a few times 10 Myr, and sufficient spin-down to slow rotation at the Hyades age. It must be emphasized that, within the framework of our admittedly simple model, this choice of parameters is close to unique. The short coupling timescale is necessary to produce the spread in rotational velocity, and influences the spin-down. The dynamo saturation is required to maintain a considerable spread in rotation rate at least until the age of the $\alpha$ Persei cluster. The high level of the saturation ($Q_{sat} = 20$) ensures a spin-down to low rotation rates at the Hyades age. The choice of the 5 day period distinguishing faster-rotating, diskless stars from slowly rotating stars with disks recovers the right ratio (1/3 versus 2/3) of fast versus slow rotators in $\alpha$ Persei. The presence of a disk for a few million years ensures the slow rotation rates observed in the young ZAMS clusters. Quantitative comparison with observations reveals some remaining discrepancies, however. In particular, the large number of stars in $\alpha$ Persei and the Pleiades that rotate at velocities less than 10 kms$^{-1}$ is still not fully reproduced. Whether this is due to aspects of core-envelope coupling, dynamo saturation, and/or disk regulation not captured by current models, or to additional physical mechanisms not considered to date, remains very much an open question. More conclusive tests of present analyses of rotational evolution will eventually result from more complete observations of rotational velocities for slowly rotating stars in these clusters. It is also clear that observations of more clusters of different ages will improve our understanding of the angular momentum evolution. In particular, late PMS clusters (ages of $\sim$ 30 Myr) must show whether the rapid spin-down of stars (due to the temporary core-envelope decoupling) indeed occurs in the timescales considered (about 10 Myr), since relevant differences can be expected in the distributions of the rotational velocities.

*Acknowledgements.* R.K. thanks the staff of the High Altitude Observatory in Boulder, for its warm hospitality during his visits, and the Belgian National Fund of Scientific Research, for granting him the opportunity to visit. The authors thank Li Jianke for reading the manuscript. We thank Dr. J.R. Stauffer for very useful comments on our first writing of the manuscript, and the referee, Dr. J. Bouvier, for an extensive and most helpful report.

## Appendix A: Weber-Davis (WD) model for the solar wind

The large scale dynamics of the solar wind can be modeled qualitatively using an MHD (magnetohydrodynamic) description of the solar wind plasma in the corona and beyond. The 'quiet' solar wind is then modelled as a stationary state, in which plasma properties at the coronal base (Temperature $T_o \simeq 1.5 \times 10^6$ K, number density $N_o \simeq 10^8 cm^{-3}$, rotating with angular velocity $\Omega_\odot \simeq 3 \times 10^{-6}\ s^{-1}$, magnetic field $B_\odot \simeq 2$G) are linked with interplanetary properties by means of a transonic, trans-Alfvénic continuous plasma outflow. The Weber-Davis wind solution (Weber & Davis 1967) solves for the steady-state ($\partial/\partial t = 0$) expansion of the solar corona using an axisymmetric ($\partial/\partial\phi = 0$) and polytropic ($p/p_o = (\rho/\rho_o)^\alpha$, where $p$ is the pressure, $\rho$ is the density, and $\alpha$ is the polytropic index) description in the equatorial plane ($\partial/\partial\theta = 0$, $v_\theta = 0$, where $\theta$ is the spherical polar angle). In this picture, the mass flux ($4\pi r^2 \rho v_r$) and the magnetic flux ($4\pi r^2 B_r$) are constant, and the magnetic field is linked with the velocity components ($v_r$, $v_\phi$) through flux freezing ($\nabla \times (\boldsymbol{v} \times \boldsymbol{B}) = \mathbf{o}$). We constructed a 'reference' present day sun WD solution for a polytropic index $\alpha = 1.13$ and the physical properties stated above at a 'base' level of $r_o = 1.25 R_\odot$. A WD solution is characterized by the existence of three critical points, where the plasma flow speed equals a characteristic magnetosonic or Alfvén speed. For the 'reference' present day sun solution, these critical points are at $r_s = 9.2 R_\odot$ (the slow magnetosonic point), $r_A = 36.5 R_\odot$ (the Alfvén point) and at $r_f = 39.1 R_\odot$ (the fast magnetosonic point). Radial flow speeds at these radii are, respectively 100 kms$^{-1}$, 190 kms$^{-1}$ and 194 kms$^{-1}$, whereas the radial base expansion velocity is only 2.3kms$^{-1}$. For comparison, the coronal base soundspeed $a_o$ is about 167kms$^{-1}$. The radial plasma speed at 1AU ($215 R_\odot$) works out to be about 263kms$^{-1}$ (and $v_\phi = 3.67$kms$^{-1}$), with a proton density of about $15 cm^{-3}$ and temperature of $2.128 \times 10^5$ K, in qualitative agreement with the observations and in quantitative agreement with the properties of the low-speed solar wind as described by Withbroe (1988). The acceleration of the solar wind plasma to this super(magneto)sonic, superAlfvénic speed at 1AU is caused mainly by the pressure gradient associated with the hot corona.

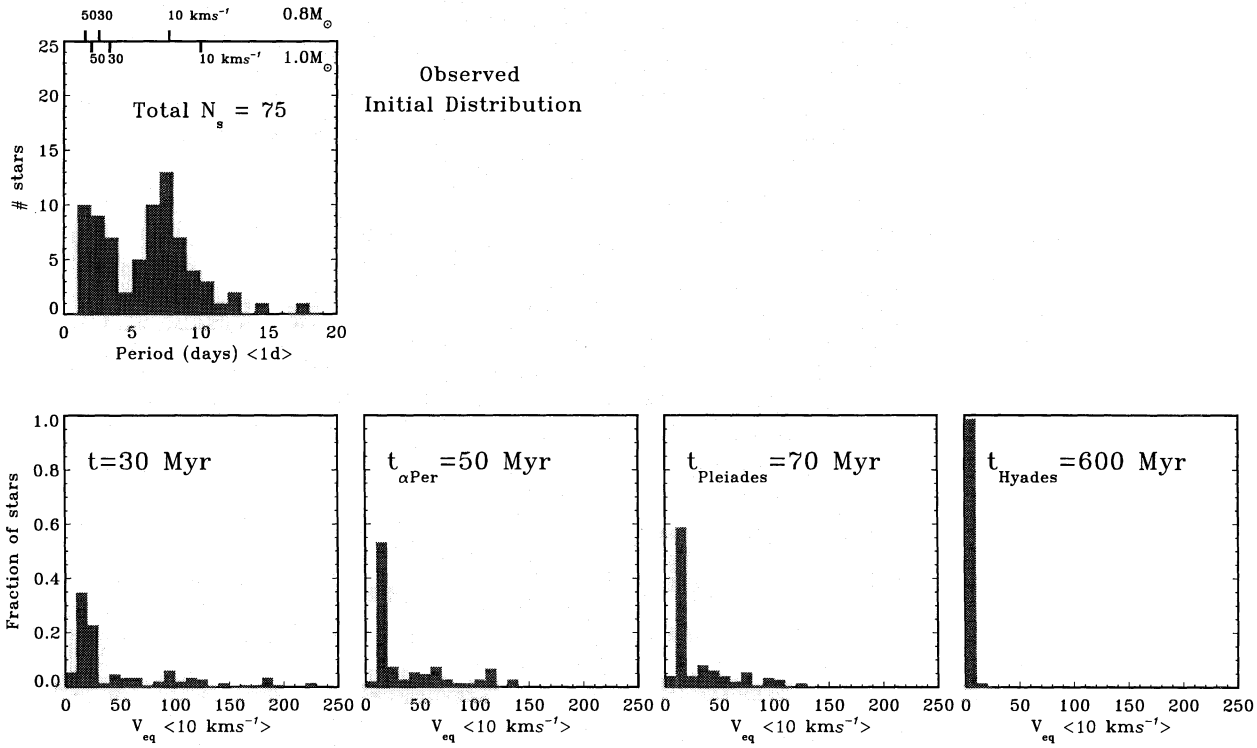


**Fig. 9.** The observed bimodal distribution of rotation periods for young PMS stars (data compiled from a variety of sources: Walker 1990; Mandel & Herbst 1991; Attridge & Herbst 1992; Bouvier et al. 1993), and its subsequent evolution, shown as a frequency distribution in equatorial rotational velocity. Velocity bins are of width 10 kms$^{-1}$. The parameters used for the evolution are: $\tau_c$ = 10 Myr, $Q_{sat}$ = 20. Stars with initial period longer than 5 days have a circumstellar disk for 4 Myr beyond $t_{RC}$, and the distributions shown have equal numbers of 0.8 and 1.0 solar mass stars

The angular momentum loss in the solar case is almost entirely due to the torque associated with the magnetic stresses with little contribution (at the $< 10$ % level) from advection of angular momentum. The (net) specific angular momentum loss rate $L$, calculated from this model, is equivalent to strict corotation of the plasma out to $r_A$:

$$L = \Omega r_A^2.$$

The total rate of change of the solar angular momentum is then given by

$$\frac{dJ_\odot}{dt} = \frac{2}{3}\Omega r_A^2 \dot{M} = 0.24 \times 10^{32} (dyne\, cm), \quad (8)$$

where $\dot{M} \sim 2.94 \times 10^{-14} \mathrm{M}_\odot yr^{-1}$ is the mass loss rate. The resulting time-scale for angular momentum loss is

$$\tau_{w,\odot} = \frac{J_\odot}{\dot{J}_\odot}. \quad (9)$$

In general, the WD model for a stellar wind can be characterized by the set of parameters (see e.g. Belcher & MacGregor 1976)

$$\begin{aligned} c_1 &= \alpha(1.13) \\ c_2 &= a_o(167 km/s) \\ c_3 &= \Omega r_o/a_o = (\Omega/\Omega_\odot)(R_*/R_\odot)c_{3,\odot} \\ c_4 &= \sqrt{2GM_*/r_o}/a_o = \sqrt{(M_*/\mathrm{M}_\odot)/(R_*/R_\odot)}c_{4,\odot} \\ c_5 &= A_{ro}/a_o = (B_*/B_\odot)c_{5,\odot}. \end{aligned}$$

For all the stellar models ($0.8\mathrm{M}_\odot$, $0.9\mathrm{M}_\odot$ and $1\mathrm{M}_\odot$) considered in this paper, the factor $\sqrt{(M_*/\mathrm{M}_\odot)/(R_*/R_\odot)}$ stays within the narrow range [0.7,1.1], throughout the entire evolution (from $t_{RC}$ till the solar age). Therefore, when calculating the instanteneous braking timescale $\tau_w$ for a low mass star from the WD wind model, it suffices to update the present day solar solution (as described above) for the changes in the centrifugal ($c_3$) and magnetic ($c_5$) parameters. We then additionally assume that the solar coronal base temperature ($T_o$) and density ($N_o$) are reasonable estimates for the coronal conditions of such low mass stars. We emphasize that the centrifugal and magnetic parameters are significantly influenced by the structural evolution, through the varying stellar radius (factor $R_*/R_\odot$ for $c_3$ and $(R_*(t_\odot)/R_*)^2$ for $c_5$).

We have calculated WD wind models for centrifugal parameters ranging from 0.5 to 60 times $c_{3,\odot}$, and magnetic parameters from 0.5 to 60 times $c_{5,\odot}$. This table of solutions can then be used to calculate the angular momentum loss rate $dJ/dt$ for a low mass star at any time during its evolution, taking into account the changes in surface gravity (influenced by $M_*$ and $R_*$), rotation rate ($\Omega$) and base coronal field ($B_*$, which is linked to the star's rotation rate by the assumed dynamo law $B_*(\Omega)$). In Fig. 10, the angular momentum loss rate calculated for a $1\mathrm{M}_\odot$, $1R_\odot$ star is shown as a function of the stars rotation rate, for both linear and saturated dynamo's ($Q_{sat}$ = 5 and 10). At low rota-

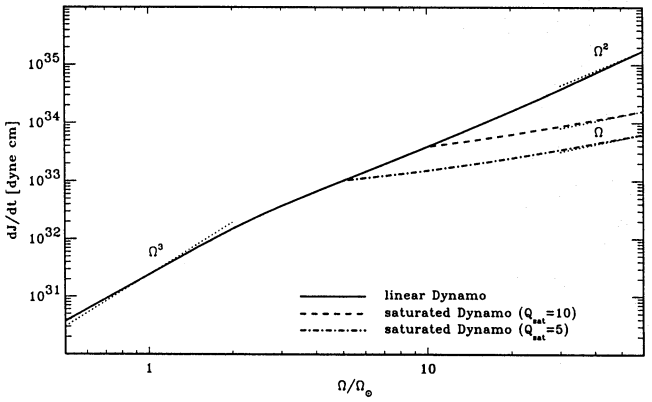


**Fig. 10.** The wind-induced torque (in dyne cm) as calculated from a Weber-Davis stellar wind model, for a $1M_\odot$, $1R_\odot$ star, as a function of the surface rotation rate ($\Omega$ in $\Omega_\odot$ units). The solid line is for field strengths linearly increasing with rotation rate. The dashed line is for a field saturating when the star rotates faster than $10 \times \Omega_\odot$, and the dash-dotted line is for saturation at $5 \times \Omega_\odot$. The dotted lines are power-law fits $\dot{J} \propto \Omega^n$, valid at low and high rotation rates

tion rates, the angular momentum loss rate $\dot{J} \propto \Omega^3$, while fast rotation is consistent with a $\dot{J} \propto \Omega^2$ for the linear dynamo and $\dot{J} \propto \Omega$ for the saturated dynamo's. These power laws however are poor representations of the true $\dot{J}(\Omega)$ and we therefore only rely on their approximate estimates when we need to extrapolate out of our constructed table of WD solutions.

In Fig. 11, we show the rotational evolution of a solar mass star, with initial equatorial velocity 15 $\mathrm{kms}^{-1}$ and $\tau_c = 20$ Myr, for a linear dynamo, with and without the incorporation of the gravitational effects from the varying stellar radius. The braking timescale calculated from the WD model shows that especially during the early PMS evolution, gravitational effects play an important role in the determination of the changing wind characteristics.

section*Appendix B: a model for magnetically coupled disk accretion

The interaction between a contracting, PMS star and a surrounding, magnetized accretion disk has been suggested as a means of accounting for the observed bimodality (WTTS/CTTS) in the period distribution of TTS. CTTS show evidence for surrounding disks, and rotate slower, on average, than the presumably diskless WTTS. It thus seems possible that the disk interacts magnetically with the star, and effectively 'locks' the rotation rate of the star, even though the star is contracting. Quantitative modelling of this disk-locking process is a formidable task, and in the present paper, we have chosen to adopt the crudest 'model' possible, namely, to assume that when a disk is present (for timescales of the order of 5 Myr), the net torque applied to the convection zone is of precisely the magnitude required to produce a constant rotation period. In this Appendix, it is shown that for 'reasonable' values of the physical parameters during the accretion phase of a young PMS star, this assumption can capture the essential behaviour of the surface rotation rate.

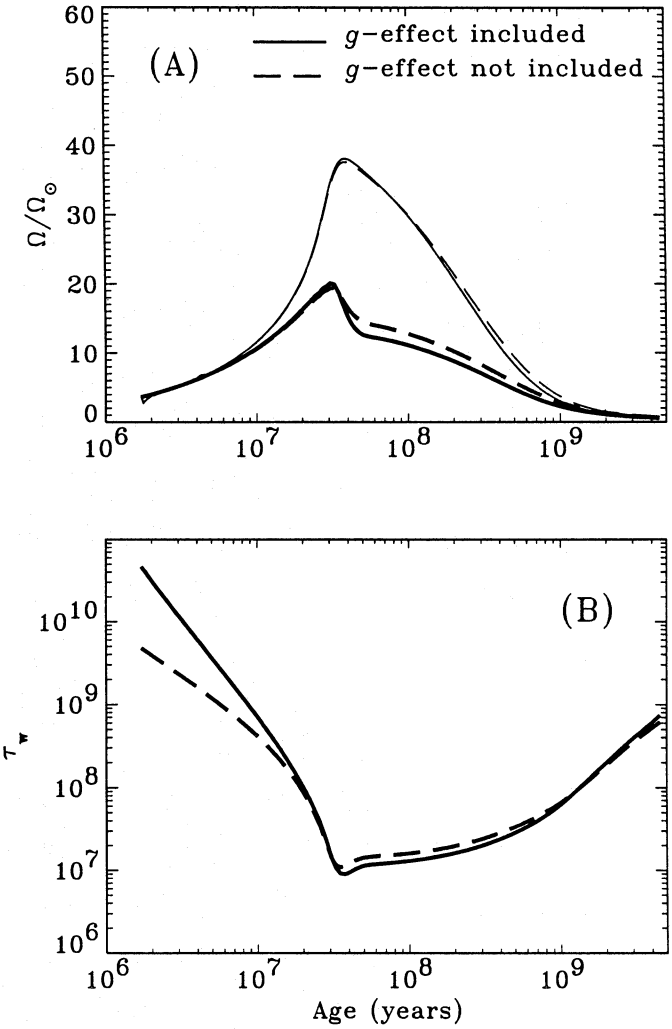


**Fig. 11a and b.** The evolution of the rotation rate of core (thinner lines) and envelope (Panel **a**) for a solar mass star, with $\tau_c = 20$ Myr, a linear dynamo, and initial equatorial velocity $V_{eq} = 15$ $\mathrm{kms}^{-1}$, with (solid line) and without (dashed line) the incorporation of the gravitational effects on the wind braking timescale $\tau_w$. The braking timescale is plotted in Panel **b**

To quantify the accretion phase of a magnetic TTS, we use the model developed by Collier Cameron & Campbell (1993). Specific details of this model can be found therein. Here, we restrict ourselves to repeating the assumptions incorporated in the model. It is assumed that the stellar disk is Keplerian (angular velocity $\Omega_K$), and embedded in a magnetosphere, which corotates rigidly with the surface angular velocity of the star. At the disk surface, the poloidal magnetic field of the star is then sheared at a rate proportionate to the local angular velocity difference. A steady-state is reached when the dissipation that occurs in the disk (e.g. by magnetic buoyancy or turbulence) is balanced by this inductive production of toroidal field. At the corotation radius $R_{co}$ (i.e., the radius at which $\Omega_* = \Omega_K$), the ratio of the vertical integrals of the magnetic and viscous force densities changes sign. Inside $R_{co}$, both forces act in the same direction, while for $r > R_{co}$, the force ratio is negative. The

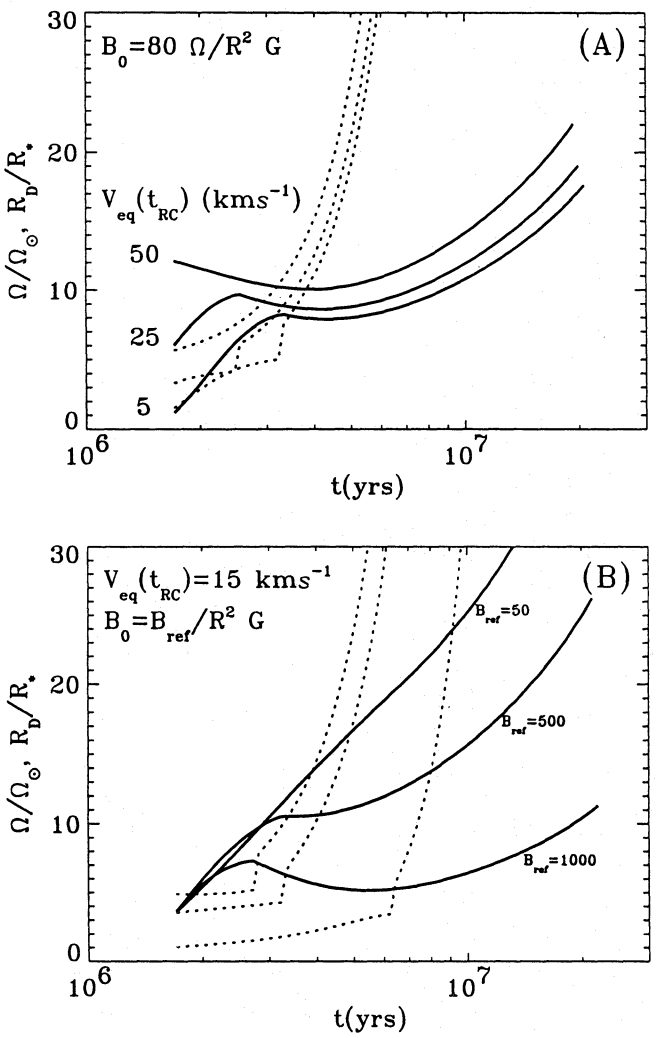


**Fig. 12a and b.** The evolution of the surface rotation (solid lines) and radial position of the disruption radius (dotted lines) of a solar mass star using the Cameron-Campbell model, from $t_{RC}$ up to 20 Myr. This model takes into account: (i) structural evolution; (ii) disk accretion; and (iii) magnetic coupling with the surrounding disk. In Panel **a**, we vary the initial equatorial rotational velocity, and assume a dynamo magnetic field $B_0 = 80\Omega/R^2$ G. In Panel **b**, the initial rotation is 15 kms$^{-1}$, and the field prescription is varied as $B_0 = B_{ref}/R^2$ G. In both panels, $\tau_c$ = 20 Myr, $\tau_{acc}$ = 1 Myr and the total accreted mass is $M_{acc} = 0.05M_\odot$

inner boundary of the disk is taken to be located at the radial position $r = R_D$, where the force ratio exceeds the value 2. Interior to $r = R_D$, it is assumed that the highly-conducting stellar magnetosphere is entered, and the disk is disrupted. The disruption radius $R_D$ can occur outside the corotation radius, in which case it is assumed that the accretion of disk material onto the star is too weak to cause any significant spin-up. Significant accretion takes place when the disruption radius lies within the corotation radius, and the accreting torque is taken to be

$$T_A = \dot{M} R_D^2 \Omega_K(R_D), \qquad (10)$$

where $\dot{M}$ is the mass accretion rate. The magnetic torque acting on the star depends on whether or not disk disruption occurs inside or outside the corotation radius. If disruption occurs inside $R_{co}$, the magnetic torque has a spin-up and a spin-down contribution. If it occurs outside $R_{co}$, the magnetic torque only brakes the star's rotation.

In Fig. 12, we show the evolution of the surface rotational velocity (solid lines), together with the evolution of the disruption radius (dotted lines), calculated for some different prescriptions for the photospheric magnetic field strength. In both panels, we use a 1 $M_\odot$ star, with a coupling timescale of $\tau_c$ = 20 Myr, and evolve it up to an age of about 20 Myr using the model for disk accretion described above. The total mass accreted is taken to be $0.05M_\odot$, and the accretion rate $\dot{M}$ is taken to diminish exponentially in time with a characteristic timescale $\tau_{acc}$ = 1 Myr. In panel (A) we show the angular velocity of the stellar surface and the disk disruption radius as functions of time, for three values of the initial equatorial rotational velocity (5 kms$^{-1}$, 25 kms$^{-1}$ and 50 kms$^{-1}$). For these solutions, the field strength used to determine the position of the disruption radius is given by a linear dynamo law, $B_0 = 80(\Omega_*/\Omega_\odot)/(R_*/R_\odot)^2$ Gauss. Under these conditions, one can see that *on average*, the surface rotation rate remains constant for about 5 Myr, after which the star spins up as a result of its overall contraction. The evolution of the disruption radius shows that *in detail* a faster spin-up occurs as long as accretion dominates (for the star initially rotating at 50 kms$^{-1}$, the disruption radius is already outside the corotation radius at $t_{RC}$ and no significant accretion takes place). Eventually however, the dynamo field becomes strong enough to disrupt the disk outside the corotation radius (discontinuous jumps in the dotted lines), and the magnetic torque spins the star down. In panel (B), we take the initial equatorial velocity of the solar mass star to be 15 kms$^{-1}$, and vary the stellar magnetic field strength by considering different values for the reference field strength $B_{ref}$ in the prescription $B_0 = B_{ref}/(R_*/R_\odot)^2$ Gauss. For a reference field $B_{ref}$ = 1000, a behavior similar to that described above is found, but when the field strength is lowered by an order of magnitude, accretion dominates the evolution for a longer time. As a consequence of this, the spin-up for $B_{ref}$ = 50 is more efficient than that due to contraction alone.

## References


Attridge,J.M.,Herbst,W. 1992, ApJ 398, L61

Belcher,J.W.,MacGregor,K.B. 1976, ApJ 210, 498

Bouvier,J. 1991, in: '*Angular Momentum Evolution of Young Stars*', p.41, eds. S. Catalano & J.R. Stauffer, Kluwer Academic Publishers, Dordrecht

Bouvier,J., Cabrit,S., Fernández,M., Martín,E.L., Matthews,J.M. 1993, A&A 272, 176

Bouvier,J. 1994, in: '*Eight Cambridge Workshop on Cool Stars, Stellar Systems, and the Sun*', ASP Conf. Ser., ed. J.-P. Caillault, in press

Charbonneau,P.,MacGregor,K.B. 1993, ApJ 417, 762

Collier Cameron,A.,Campbell,C.G. 1993, A&A 274, 309

Edwards,S.,Strom,S.E.,Hartigan,P.,Strom,K.M., Hillenbrand,L.A., Herbst,W., Attridge,J., Merrill,K.M., Probst,R., Gatley,I. 1993, Astron. J. 106, 372
Ghosh,P.,Lamb,F.K. 1979, ApJ 232, 259
Ghosh,P.,Lamb,F.K. 1979, ApJ 234, 296
Hoyle,F. 1960, QJRAS 1, 29
Iben,I. 1965, ApJ 141, 993
Kawaler,S.D. 1988, ApJ 333, 236
Königl,A. 1991, ApJ 370, L39
Li,J.,Collier Cameron,A. 1993, MNRAS 261, 766
Li,J. 1994, in preparation
MacGregor,K.B.,Brenner,M. 1991, ApJ 376, 204
MacGregor,K.B. 1991, in: '*Angular Momentum Evolution of Young Stars*', p. 315, eds. S. Catalano & J.R. Stauffer, Kluwer Academic Publishers, Dordrecht
MacGregor,K.B.,Charbonneau,P. 1994, in: '*Eight Cambridge Workshop on Cool Stars, Stellar Systems, and the Sun*', ASP Conf. Ser., ed. J.-P. Caillault, in press
Mandel,G.N.,Herbst,W. 1991, ApJ 383, L75
Mestel,L.,Spruit,H.C. 1987, MNRAS 226, 57
Mestel,L.,Weiss,N.O. 1987, MNRAS 226, 123
Pinsonneault, M.H., Kawaler, S.D., Sofia, S., Demarque, P. 1989, ApJ 338, 424
Prosser,C.F. 1992, AJ 103, 2, 488
Prosser,C.F. 1994, AJ 107, 4, 1422
Skumanich,A.,MacGregor,K.B. 1986, Adv. Space Res. 6, 151
Soderblom,D.R.,Stauffer,J.R.,Hudon,J.D.,Jones,B.F. 1993, ApJS 85, 315
Soderblom,D.R.,Stauffer,J.R.,MacGregor,K.B.,Jones,B.F. 1993, ApJ 409, 624
Spiegel,E.E.,Zahn,J.-P. 1992, A&A 205, 106
Stauffer,J.R. 1994, in: 'Proceedings of the First International Conference on Circumstellar Habitable zones', ed. L. Doyle, in press
Stauffer,J.R.,Caillault,J.-P.,Gagné,M.,Prosser,C.F.,Hartmann,L.W. 1994, ApJS 91, 625
Tassoul,J.L. 1978, '*Theory of Rotating Stars*', p. 167, Princeton Univ. Press, Princeton
Tassoul,J.L.,Tassoul,M. 1989, A&A 213, 397
Vilhu,O. 1984, A&A 133, 117
Walker,M.F. 1990, PASP 102, 726
Weber,E.J.,Davis,L. 1967, ApJ 148, 217
Withbroe,G.L. 1988, ApJ 325, 442

This article was processed by the author using Springer-Verlag LaTeX A&A style file version 3.